

1 Effect of non-uniform illumination and temperature distribution  
2 on concentrating solar cell - A review

3

4 Guiqiang Li<sup>1\*</sup>, Qingdong Xuan<sup>1</sup>, Gang Pei<sup>1</sup>, Yuehong Su<sup>2\*</sup>, Jie Ji<sup>1</sup>

5 <sup>1</sup>*Department of Thermal Science and Energy Engineering, University of Science and  
6 Technology of China, 96 Jinzhai Road, Hefei City 230026, China*

7 <sup>2</sup>*Institute of Sustainable Energy Technology, University of Nottingham, University  
8 Park, Nottingham NG7 2RD, UK*

9

10 **Abstract**

11 Concentrated photovoltaic (CPV) technology as a typical PV application is  
12 becoming popular due to its advantages of high conversion efficiency and low cost etc.  
13 However an important issue for CPV technology is the non-uniformity on the  
14 illumination and the temperature which can finally influence the overall electrical  
15 efficiency of solar cells. This study presents the feature of the non-uniform  
16 illumination and temperature, and reviews the cause and harm of the non-uniform  
17 illumination and temperature. Then the specific effect on cell parameters of different  
18 solar cells is analyzed, and finally the improving methods for reducing this negative  
19 effect on concentrating solar cells are proposed. This review will help researchers to  
20 learn the effect of the non-uniformity on the illumination and the temperature, and  
21 common improvement method, which will benefit CPV design and optimization.

22

23 **Keywords:** non-uniform illumination; concentrating solar cell; non-uniform  
24 temperature; cooling technology

25

26 \*Corresponding authors. Tel/Fax: +86 551 63607367. E-mail: ligq@mail.ustc.edu.cn;  
27 Yuehong.Su@nottingham.ac.uk

## 28 **Contents**

29	Abstract .....	1
30	1. Introduction.....	3
31	2. Concentrating solar cell overview .....	5
32	2.1 Difference from traditional solar cells .....	6
33	2.2 Current Cell models .....	7
34	3. Effect of non-uniform illumination on CPV solar cells.....	9
35	3.1 Characteristics of the non-uniform illumination .....	10
36	3.2 Cell parameters analysis under non-uniform illumination.....	11
37	3.2.1 Localized illumination .....	11
38	3.2.2 Shaded cell.....	16
39	3.3 Methods to alleviate the effect .....	17
40	3.3.1 Cell structure.....	18
41	3.3.2 Concentrator choice .....	19
42	4. Effect of non-uniform temperature on solar cells .....	21
43	4.1 Characteristics of the non-uniform temperature.....	21
44	4.2 Cell parameters analysis under non-uniform temperature .....	22
45	4.2.1 Temperature distribution profile.....	22
46	4.2.2 Variation of cell parameters .....	23
47	4.3 Improvement methods.....	25

48	4.3.1 The traditional cooling methods .....	27
49	4.3.2 The new cooling technology.....	28
50	5. Dual effect.....	30
51	6. Conclusion .....	34
52	Acknowledgement .....	35
53	References.....	35

54

55 **1. Introduction**

56 Energy is one of the vital factors for any country development. Till date the coal  
57 as one of the major sources of electricity production has the share of electricity by 42%  
58 and it will still be the main source of electricity in many countries in the next few  
59 decades [1]. But the problems of worldwide energy shortage and environment  
60 pollution are becoming more serious, so renewable energy has been encouraged by  
61 many countries due to the advantages of being sustainable and not contributing to the  
62 world's  $CO_2$  greenhouse gas emissions [2]. Solar energy as an abundant and large  
63 potential renewable energy source in the world has no pollution [3], so it has been  
64 widely used. According to 2015's data, solar photovoltaics (PV) contribute about 227  
65 GW, and concentrating solar power (CSP) technologies contribute about 4.8 GW in  
66 electricity generation capacity [4]. However, the major limitation of PV technology  
67 still remains at lower performance price ratio compared to the conventional power  
68 generation techniques. Only part of the solar radiation can be converted into the  
69 electricity while the remaining solar radiation is either converted into the heat or is

70 reflected back [5]. Concentrating photovoltaic (CPV) can overcome these problems  
71 because of its lower cost and higher electrical efficiency [6]. The expensive PV  
72 material is replaced by lower cost mirrors and/or lenses, reducing the system cost but  
73 maintaining the total value of the energy captured [7]. If the cell cost can be reduced  
74 to be a small portion of the whole system cost, it can be advantageous to employ a cell  
75 with a higher efficiency, making the investment in the optics more valuable [8].  
76 Although with the concentration ratio increasing the solar cell temperature will  
77 increase, which will lead to the PV efficiency and lifespan decrease, this problem can  
78 be solved by using a proper cooling technology [9]. In addition, the  
79 photovoltaic/concentrated solar power hybrid system can attain the better power  
80 quality electricity compared to the PV-alone system [10].

81

82 Concentrating solar cell is the core part of a concentrating photovoltaic system.  
83 There are many kinds of solar cells, about 90% of which are monocrystalline and  
84 multi-crystalline silicon solar cells [11], and others include III–V compound solar  
85 cells (such as single-junction GaAs and multi-junction concentrators), thin film cells  
86 (such as cadmium telluride (CdTe) thin-film photovoltaics, copper indium gallium  
87 diselenide (CIGS) solar cells, and amorphous silicon cells, dye-sensitized solar cells,  
88 organic solar cells, etc. [12] and since 1960 semiconductors (III–V and II–VI) based  
89 solar cells were studied and new technology for polycrystalline Si (pc-Si) and  
90 thin-film solar cell have been establish in order to lower the material cost and energy  
91 input but increase the production capacity [13]. Silicon wafer-based solar cells are

92 believed as 'first generation' while 'second generation' are lower cost thin-film solar  
93 cells, and the concentrating solar cell was regarded as the third generation solar cells  
94 [14]. There are two ways to widen the application of solar cells: one is to decrease the  
95 costs, but many ways have been tried on this [15] and it can't achieve an effective  
96 progress in a short period of time, and the other is to improve the efficiency of the  
97 cells, which has also become the focus of the study of concentrating photovoltaic.

98       However, there are several factors that can affect the efficiency of cells in the  
99 CPV system, such as the kind of cells, concentration ratio, non-uniform illumination,  
100 non-uniform temperature, cooling structure and so on. In this paper, the main purpose  
101 is to summarize the effect of non-uniform illumination and non-uniform temperature  
102 on concentrating solar cells, and to analyze the performances on different cells and to  
103 illustrate the improvement methods to overcome the negative influences.

104

## 105 **2. Concentrating solar cell overview**

106       Solar cell is the core component of the CPV system, and its characteristic plays  
107 an important role on the overall performance of the CPV system. Low concentration  
108 photovoltaic (LCPV) systems can adopt the conventional high performance silicon  
109 solar cells [16] which can be used under the concentration ratio of 2 to 10 suns [17].  
110 But for medium and high solar concentrating PV systems, because of the high  
111 operating temperature of cell which will influence its several parameters, it needs the  
112 specially designed solar cells which could further employ the sun-tracking device and  
113 cooling technique [18]. Medium and high concentrator PV technology is still in a

114 deployment stage [19]. Silicon-based solar cells may be not much proper, and III–V  
115 multi-junction solar cells are more suitable for the solar concentrating system because  
116 of the lower base electrical resistivity [20]. Multi-junction solar cells used for CPV  
117 systems could deliver the electrical power with a lower cost compare to the traditional  
118 one [21] and the PV conversion efficiency will increase with a high solar  
119 concentration ratio until the series resistance limits the performance [22]. Xing et al.  
120 [23] used finite element method to calculated the thermal performance of silicon  
121 vertical multi-junction (VMJ) solar cell under 1D non-uniform illumination of 500  
122 suns, and used SPICE software to calculated the PV electrical performance based on  
123 the thermal simulation results and founded that it had a better performance than  
124 silicon planar junction cell under the same conditions of 500 suns which means  
125 multi-junction solar cells have a good potential in CPV. In recent years, the electrical  
126 efficiency of the III–V triple-junction solar cells has been increased significantly [24],  
127 and according to Ref. [25], [26], [27], the highest efficiency can reach 28.3% [25], 40%  
128 [26], and 41.1% [27].

129

## 130 2.1 Difference from traditional solar cells

131 The computing and testing of traditional cells are carried out under the  
132 assumption of the uniform condition, and the deviation is acceptable for the practical  
133 application. However, for concentrating photovoltaic cells, especially with the  
134 increase of solar concentration ratio, the non-uniformity can cause a significant  
135 difference on different solar cells with the decline in the overall performance. So in

136 the analysis of the concentrating solar cells, the effect of non-uniformity on cells has  
137 the great significance. And in the process of analysis, there is a lot of limitations when  
138 using the analysis methods of traditional cells, since the characteristics of the  
139 concentrating solar cell itself must be taken into consideration. For example, using the  
140 light intensity and temperature function with a Gaussian distribution takes the place of  
141 that with the uniform distribution; or using a 2-d or 3-d cell model replaces the one  
142 dimensional diode model.

143

## 144 2.2 Current Cell models

145 The traditional parallel circuit model consists of the diode and the current source  
146 is widely used to characterize the electrical characteristics of solar cells. But high  
147 concentration solar cells have specific characteristics different from those of  
148 conventional flat-plate solar cells [28]. The traditional model ignores the  
149 non-uniformity of light intensity and temperature on the cell, but this influence on the  
150 CPV cells has become very significant. Also, different illumination spectra, angles of  
151 impinging light and chromatic aberrations should be taken into consideration [29]. So  
152 in order to increase the performance of such concentrating solar cells, a modeling as  
153 accurate as possible is necessary to achieve realistic results [30]. The circuit network  
154 model to analyze the solar cell electrical characteristics under non-uniformity can be  
155 used. In recent years, the scientists have also devoted considerable efforts in  
156 developing models that reproduce the electrical behavior of solar concentrating under  
157 different operating conditions [28]. The important issue of establishing the model is to

158 minimize the series resistance due to the loss of the voltage caused by large generated  
 159 currents. And when a cell is designed for concentration, the design of the front metal  
 160 grid spacing is important to reduce the resistance of the emitter region.

161 Franklin and Coventry designed a two-dimensional cell model under an average  
 162 concentration ratio of 20-50 suns, and the net generated intensity is given by Eq. (1)  
 163 [31]. Generated current was considered to gradually vary only in the x-direction and  
 164 the emitter resistance could result in a junction voltage that increases with the distance  
 165 from the finger.

$$166 \quad I_j(x, y) = I_0(x, y) \left( e^{\frac{q \cdot V_j(x, y)}{k \cdot T(x, y)}} - 1 \right) - I_L(x, y) \quad (1)$$

167 where  $I_j(x, y)$ ,  $I_0(x, y)$ ,  $I_L(x, y)$ ,  $V_j(x, y)$ ,  $T(x, y)$  stand for the net current flowing  
 168 across the junction, the reverse saturation current, the photocurrent, the p-n junction  
 169 voltage and the temperature respectively for the given element position  $(x, y)$ .

170

171 Mellor, et al. presented another two-dimensional model of the current  
 172 distribution in the front surface of the cell which took into account the distributed  
 173 diode effect [32]. The cell model can be seen as consisting of a series of the same  
 174 fingers and it doesn't limit the vertical current flowing from the emitter to the fingers.

175 The illumination intensity falls on the PV cell is given by:

$$176 \quad G(x) = G_0 A_0 \exp\left(-\frac{x^2}{2s_0^2}\right) \quad (2)$$

177 And the current generated in the emitter region is given by:

$$178 \quad Q_j = C_1 G + C_2 T^3 \exp\left(\frac{-E_g}{k_b T}\right) \left[ \exp\left(\frac{q_e V_j}{n k_b T}\right) - 1 \right] \quad (3)$$



179 While in the dark finger and bus-bar region is given by:

$$180 \quad Q_j = C_2 T^3 \exp\left(\frac{-E_g}{k_b T}\right) \left| \exp\left(\frac{q_e V_j}{n k_b T} - 1\right) \right| + C_3 V_j \quad (4)$$

181  $G_0$  is the mean illumination across the cell,  $S_0$  controls the width of the curve;  $T$   
182 is the cell temperature;  $V_j$  is the junction electric potential;  $q_e$  is the electron charge,  $k_b$   
183 is the Boltzmann constant;  $E_g$  is the bandgap energy;  $n$  is the diode ideality factor, and  
184  $C_1$ ,  $C_2$  and  $C_3$  are coefficients specific to a given cell.

185

186 A useful 3D model based on the distributed circuit units for concentrating solar  
187 cells was established by Galiana, et al. [33] which had a greatly improvement  
188 compared with the conventional model [34] in greater detail. The model considered  
189 the various influence factors, such as all of the series resistances and even the parallel  
190 resistances. The whole solar cell could be modeled based on the electrical circuit  
191 attained by the interconnection of every unit circuit. There are three main types of  
192 elementary units in the model [33]: (a) illuminated area; (b) dark area (bus bar and  
193 front grid); and (c) perimeter region. The equivalent circuit for the illuminated areas is  
194 the only unit where photo-generation takes place and that for the dark areas (beneath  
195 the busbar and fingers) considers the recombination in the neutral regions as well as in  
196 the depletion region with two diodes. The equivalent circuit for the perimeter regions  
197 (beneath the busbar) has basically the same electrical circuit concerning in the ohmic  
198 losses.

199

### 200 **3. Effect of non-uniform illumination on solar cells**

### 201 3.1 Characteristics of the non-uniform illumination

202 In CPV systems, concentrators are used to concentrate the sunlight on solar cells.  
203 It is hoped that the illumination is uniform, but in reality, a part of the area of solar  
204 cells may be accepted by the excessive light, or rarely be exposed to the light.

205 There are two distinctive features of the non-uniformity: a single solar cell with  
206 the non-uniform illumination or a series of cells connected together with different  
207 illumination on each cell surface [35]. In the first case, some parts of a single cell  
208 surface be illuminated and some are rarely illuminated, so the part which accepts  
209 excessive exposure to the light may generate the huge current and heat. In the second  
210 case, because the cells in the CPV system often exist in series, and one shaded could  
211 affect the whole system, causing the system performance to decrease significantly and  
212 leading the cell to damage due to reverse-bias operation and overheating [36]. Solar  
213 cells are often used in series, since each cell cannot maintain the absolute same  
214 performance, the total power output is less than the sum of individual power, which is  
215 called 'current mismatching'.

216 There are many reasons that will cause non-uniform illumination, here they are  
217 summarized below in Table 1 [31, 35, 37, 38].

218

219 From the table 1, it can be found that the concentrator optics play an important  
220 role on the illumination on cells, so the improper design may lead to severe  
221 non-uniformity. Meanwhile, unbecoming position, shading, spectral response also can  
222 cause this phenomenon. However, this non-uniformity can affect the whole CPV

223 system on the overall economic benefits, the electrical performance of the solar cell,  
224 thermal features and so on.

### 225 3.2 Cell parameters analysis under non-uniform illumination

226 Solar cells performance is mainly characterized by the four basic parameters:  
227 Short Circuit Current  $I_{sc}$ , Open Circuit Voltage  $V_{oc}$ , Fill Factor  $FF$  ( defined as the  
228 ratio of the maximum power from the solar cell to the product of  $I_{sc}$  and  $V_{oc}$  ) and  
229 the energy conversion efficiency  $\eta$ , and they will all be affected by illumination  
230 conditions. For the purpose of experimental or numerical analysis, it is difficult to  
231 reproduce a non-uniform illumination distribution caused by a real solar concentrator,  
232 so a localized illumination in experiments and a standardized illumination such as  
233 Gaussian distribution or a simulated distribution are usually employed, as detailed in  
234 the following.

#### 235 3.2.1 Localized illumination

236 It is known that there are two distinctive performances of non-uniformity in  
237 section 3.1, and the first case that the inhomogeneous illumination intensity on a  
238 single cell is analyzed here.

##### 239 ● Partitioned uniform illumination

240 In Coventry's study, a monocrystalline silicon solar cell was employed to indicate  
241 the effects of the non-uniformity on the  $I$ - $V$  characteristics experimentally [39]. An  
242 experiment was conducted on a single solar cell in two cases: 30 X concentration ratio  
243 over the whole cell, and 90 X concentration ratio over the middle third of the cell. The  
244 results showed that there is a reduction in open circuit voltage of 6.5 mV (Fig. 1) and

245 an obvious deviation of the  $I$ - $V$  curves is observed under the uniform and non-uniform  
246 illumination conditions, and the author pointed out an efficiency drop from 20.6%  
247 with uniform illumination to 19.4% with non-uniform illumination [40].

248

249 Katz et al. [41] used a 100 mm<sup>2</sup> triple-junction GaInP<sub>2</sub>/GaAs/Ge cell with the  
250 uniform front metallization under a localized illumination procedure. Solar  
251 illumination on the cell  $P_{in}$  was provided from 0.1 to 8 W. The short-circuit current  
252  $I_{sc}$  was proportional to  $P_{in}$  with a photocurrent generation ratio  $G = I_{sc} / P_{in}$ . The  $V_{oc}$ ,  
253  $FF$  and  $\eta$  will all get a decline affected by the local illumination compared with  
254 the uniform illumination. With  $P_{in}$  increase, the decline of the  $V_{oc}$ , fill factor  $FF$   
255 and dependence of energy conversion efficiency  $\eta$  will also gradually increase and  
256 the deviation values seems to be larger with  $P_{in}$  at the higher level. However,  
257 especially, the position of the local illumination on cell have little influence on the  
258 decline of the parameter  $FF$ .

259

260 Manor et al. [42] used a large photoactive area organic cell with  
261 poly(3-hexylthiophene) (P3HT)/PCBM BHJ. The cell parameters was measured  
262 under various concentrations of uniform and localized illumination. The results  
263 indicate that the localized illumination of different part over the cell area gives  
264 identical results as mentioned above using the triple-junction cell. For the  $V_{oc}$ , from  
265 Fig. 2(b), it can be seen that there exists a decline when the cell is exposed to the  
266 localized illumination and the decline has remained at about 0.1V. In addition, it is

267 clearly that the results in the localized mode show the superior  $I_{sc}$ ,  $FF$  and  $\eta$   
268 values in Fig. 2(a), Fig. 2(c) and Fig. 2(d). With the increase of light intensity,  $FF$   
269 and  $\eta$  both show the tendency of decline. This seems to be a special situation which  
270 demands more attention.

271 ● Gaussian distribution

272 In the process of modeling, the distribution profile of the non-uniform  
273 illumination needs to be confirmed. And the cell parameters can be observed by  
274 experiment after the correct choice.

275 In the cell circuit modeling analysis, most linear concentrators usually have the  
276 non-uniform illumination profiles in the finger direction, such as a Gaussian function  
277 [43]. This distribution can be instead of the actual circumstances, especially for the  
278 Fresnel lens concentrating device [44].

279 The rough graph is shown in Fig. 3 [45]. The model based on Gaussian  
280 illumination incident on the cell on the x axis, which is also the finger direction:

$$281 \quad R_g(x) = R_0 \exp\left(-\frac{(x-x_0^R)^2}{2S_R^2}\right) \quad (5)$$

282 where  $R_0$  entangles the normalisation factor which ensures the desired mean  
283 irradiance across the cell,  $x_0^R$  controls the Gaussian illumination center, and  $S_R$  is  
284 the width of the illumination curve [45].

285

286 In the study by Franklin and Coventry [31] in 2002, the solar cell efficiency  
287 reduced from 17.3% under the uniform illumination and temperature, to 16.8% under  
288 the distributed illumination and uniform temperature and the open circuit voltage

289 experiences a decline of about 5mV under the identical total illumination in each case  
290 (Fig. 4). Also, it is concluded that open circuit voltage and efficiency both experience  
291 a significant decline with increasingly centralised illumination profile (Fig. 5). This  
292 can also be proved in Algora [46]’s experiment which used the 3D model mentioned  
293 above in Section 2.2. He tested this GaAs single junction solar cell under two types of  
294 illumination: (a) a 100× uniform illumination; or (b) a non-uniform illumination going  
295 from 0 at the bus bar and linearly increasing until reaching 4000× at the center, so that  
296 the average illumination on the cell was 1000×. The  $FF$  has a decline of 0.003 and  
297 the  $\eta$  has a decline of 0.4% and the  $V_{oc}$  also experienced a decline with the increase  
298 of the non-uniformity.

299

300 Mellor et al. [32] established a two-dimensional finite element model of cell as  
301 introduced in Section 2.2. The whole cell is considered as consisting of a number of  
302 identical finger elements with identical emitter sections along each side of the finger,  
303 taking into account its corresponding busbar sectors. The model was used to compare  
304 the cell parameter under 12 suns uniform and non-uniform illumination. The  $V_{oc}$  has  
305 a reduction of 0.007V, and the  $FF$  has a 0.06 reduction and the  $\eta$  has a 1.7%  
306 reduction with a peak illumination ratio of 10X compared to those under the uniform  
307 illumination (Table 2, Fig. 6 and Fig. 7). And from the results, it can be gotten that  
308 with the increase of the peak illumination ratio, the declination of the  $FF$  and  
309 efficiency of the PV cell tends to be larger. The authors also conducted the analysis of  
310 the effect of the finger number on the  $V_{oc}$  of the cell which was founded that at

311 different peak illumination ratio, the optimised fingers varied a lot (Fig. 7). This is an  
312 interesting conclusion which provides an effective way to improve the cell structure to  
313 better suit the Gaussian illumination profiles.

314

315 Domenech-Garret [45] analyzed the cell behaviour under different conditions  
316 through the model established by Mellor A et al. [32] (Fig. 8). The model was used to  
317 get the  $I-V$  curve of a cell under a 15 suns, with three conditions: (1) Gaussian  
318 Radiation (GR) distribution together with a Gaussian temperature (GT) profile; (2)  
319 GR distribution and uniform equivalent temperature(UT); (3) both uniform radiation  
320 and uniform temperature(URT). It is pointed out that the decline of  $FF$  is 0.01 and  
321  $V_{oc}$  is 10mV under the UT situation compared to URT situation (Fig. 9).

322

323 Herrero et al. [44] investigated the performance of multi-junction solar cells  
324 under the non-uniform illumination and the result is shown in Fig. 10. The increase in  
325 the non-uniformity decreases the fill factor, which is mainly because of the increase of  
326 series resistance losses that leads to the solar cell efficiency decrease in operation.  
327 Goma et al. [47] studied the effect of concentration distribution on cell performance to  
328 calculate the fill factor  $FF$  using the c-Si solar cells. The study was conducted  
329 under various incident light intensities. The effect of non-uniform distribution tended  
330 to be larger with the decrease in irradiance (Fig.11). Araki and Yamaguchi [48]  
331 studied the concentrator cells performance under non-ideal illumination. Fig. 12  
332 shows the  $I-V$  curve under Gaussian illumination compared to that under the

333 uniform illumination using the AlGaAs/GaAs 2-junction solar cell. The deviation in  
334 the  $FF$  and the cell efficiency is very large between the Gaussian illumination and the  
335 uniform illumination.

336

### 337 3.2.2 Shaded cell

338 Segev and Kribus [36] used the vertical multi-junction cells to make an  
339 experiment under non-uniform illumination. The non-uniform illumination on the  
340 vertical multi-junction (VMJ) cells was along one direction and nearly uniform  
341 illumination along another vertical direction [49]. They simulated the CPV module  
342 performance which is made of concentrating monolithic silicon VMJ cells [50],  
343 electrically connected in parallel under non-uniform illumination produced by a  
344 parabolic dish concentrator. From the experiment, dense array CPV modules based on  
345 VMJ cells connected in parallel feature very low sensitivity to non-uniform  
346 illumination, when the homogenizer is short or even doesn't exist, the decline of the  
347 efficiency is not obvious. Modules with as high as 25 VJs in each VMJ cell have  
348 shown configuration efficiencies above 0.98 with no homogenizing optics. This  
349 capability of the VMJ cells array can lead to several practical advantages.

350 As listed in Table 1, shading is an important reason for non-uniform illumination,  
351 too. Dolara et al. [51] used the poly-crystalline and mono-crystalline PV module to  
352 investigate the influence of partial shading. Three shading scenarios are applied to the  
353 PV modules (Fig. 13). From their experiment results, the  $FF$  and  $\eta$  all get a  
354 significant reduction, especially under horizontal shading scenarios for



355 poly-crystalline PV module (Fig. 14). With the increase of degree of shading, the  
356 generated current is decreasing, too. Wang et al. [52] used the PV module to  
357 determine the effects of frame shadows in two cases: a series circuit and a parallel  
358 circuit (Fig. 15). Even the shadow area is very small, it can have a serious influence  
359 on PV modules. The parallel circuit has a better performance than series one. It should  
360 be noted that for the PV modules, the shading effect may be even much more serious,  
361 it was found that the maximum and minimum drop in short circuit current of module  
362 is observed to be 84.2% and 34.6% when the solar cells of high and low spectral  
363 response are shaded [53].

364

365 Here a comparison of the cell performance between the uniform and  
366 non-uniform illumination is listed in Table 3.

367

368 Seen from the above experiment, it can be found that non-uniform illuminations  
369 have certain influence on the solar cell parameters which cause a decline on the open  
370 circuit voltage  $V_{oc}$ , fill factor  $FF$  and efficiency  $\eta$  in most instances, so it needs to  
371 find ways to decrease the influence.

372

### 373 3.3 Methods to alleviate the effect

374 There are many methods to reduce the effects of the non-uniformity, including  
375 optimizing the design for solar cells, the concentrator optics and the tracking system  
376 etc. Among them, from the perspective of optimizing the structure of the solar cell

377 itself, firstly, the concentrator cells need to have the right size and shape depending on  
378 the illuminated region in concentrating systems [35]; secondly, the surface of the cells  
379 can be dealt with. Also, when the modular design was employed, it can reduce  
380 resistance through improving routing architecture, narrowing cells interval or  
381 strengthening the arrangement density of cells.

### 382 3.3.1 Cell structure

383 Mellor et al. [32] indicated that the optimization of the front contact pattern, by  
384 increasing the number of fingers to suit the degree of non-uniformity, can mitigate the  
385 cell efficiency decrease significantly. When the number of fingers on a cell is  
386 increased from 184 to 287 under the illumination with a peak value ratio of 10, the  
387 efficiency drop is decreased from over 1.7% to less than 0.7% compared to the  
388 uniformly illuminated cell. The influence of the front contact can also be seen. The  
389 worse the quality of the front contact, the greater the decrease in the cell parameters  
390 [46]. Silva et al. [54] indicated that the device fabrication processes is important for  
391 the solar cell efficiency. For example, the silicon surface texturing process can reduce  
392 the optical reflection by increasing the surface absorption area of the incident  
393 radiation on the cell and finally increase the cell efficiency. Another technique is  
394 called the laser grooving buried gate (LGBC) (Fig. 16). This metallization process and  
395 the connecting grid design can help the solar cell to decrease their series resistance  
396 values and increase cell efficiency under the concentrated illumination. The LGBC  
397 cells can be optimized depending on the type of the concentrating system [55]. For  
398 InGaP/InGaAs/Ge triple-junction solar cell, the solar cell's structure can be optimized

399 by changing the cell size or grid electrode pitch, for reducing the series resistance and  
400 reducing the effects of the non-uniform illumination [56].

401

### 402 3.3.2 Concentrator choice

403 The incident solar irradiance on solar cells depends mainly on the optical  
404 elements [57]. An important factor to affect the overall CPV system performance is  
405 the intensity and illumination distribution from the optical elements [58], so the  
406 choice of the concentrator will affect non-uniform illumination, too. We can promote  
407 cell efficiency through the optimization of the concentrator. For concentrator silicon  
408 solar cells, when the concentration ratio increases, the tracking and cooling system  
409 will be difficult. The luminescent concentrator is made by down converter materials  
410 and can absorb incident sunlight by the species luminescent and emitted with the  
411 high quantum efficiency. Employing the down converter materials to realize  
412 concentration could reduce the demand of tracking, because the effect of the  
413 non-uniform illumination on the luminescent concentrator was less compared to that  
414 on optical elements such as reflectors and Fresnel lens [59] so it can offer an attractive  
415 approach to combine spectral and spatial concentrations of both direct and diffuse  
416 light without the expensive tracking system [60]. The up converter materials could be  
417 placed at the bottom of the bifacial illuminated cell under concentration to further  
418 improve the efficiency [61]. In Araki et al.'s [48] study above, they also proposed a  
419 simple method to anticipate non-ideal illumination effect for concentrator cells. They  
420 found that the presence of the chromatic aberration can improve the  $FF$  of the solar

421 cell from Fig. 17 [48]. The chromatic aberration (CA) losses could be minimized by  
422 Fresnel elements that alternately focus red and blue light or use a secondary optical  
423 device [62]. Hatwaambo et al. [63] used semi-diffuse rolled reflective elements in low  
424 concentrating photovoltaic system to improve the system performance. Perez-Enciso  
425 et al. [64] proposed a method to achieve a uniform flux distribution with a  
426 multi-faceted point focus concentrator, which can be used in different types of  
427 receiver and no additional device is required to homogenize the flux. Yeh [65]  
428 illustrated the solar radiation distribution of a two-stage solar concentrator combining  
429 the Fresnel lens (FL) and the compound flat concentrator (CFC), and demonstrated  
430 the way that a 2nd stage reflector of right dimension has the function of enhancing  
431 flux intensity and uniformity at the same time. Li et al. [66] proposed a lens-walled  
432 compound parabolic concentrator (CPC) as shown in Fig. 18 [66] which has an  
433 advantage of more uniform flux distribution than mirror CPC with the same  
434 geometrical concentration ratio. They did outdoor experiment [67] and indoor  
435 experiment [68] using a lens-walled CPC PV and found that the lens-walled CPC PV  
436 still has a large value of the open circuit voltage, the short circuit current and optical  
437 efficiency at the incidence angle larger than  $15^\circ$  and a better fill-factor than mirror  
438 CPC PV which indicated their hypothesis [67]. Based on the experiment results, they  
439 further performed structure optimization by simulation and experiment [69]. They did  
440 a further research in 2014 and proposed a novel lens-walled CPC with air gap as  
441 shown in Fig. 19 which set an air gap with the lens structure and maximize the total  
442 internal reflection [70]. This structure can improve optical efficiency by more than 10%

443 and is more uniform compared to the original lens-walled CPC [71].

444

#### 445 4. Effect of non-uniform temperature on solar cells

##### 446 4.1 Characteristics of the non-uniform temperature

447 Non-uniform temperature indicates that the cell temperature is different among  
448 different parts. It can be arisen by several reasons, such as the non-uniform  
449 illumination, the inconsistency of each cell, the cooling mechanism and so on. And it  
450 often cause the excessive temperature which is harmful to the solar cell and the whole  
451 system.

452 Non-uniform temperature distribution can affect the PV system performance in  
453 two ways: (1) cells efficiency loss due to power output loss; (2) the thermal fatigue  
454 induced by temperature variation because of large amount of the thermal cycles and  
455 stresses [72].

456 When a cell is exposed to the non-uniform illumination, the effect of the  
457 non-uniform solar radiation distribution will significantly lead to the temperature  
458 distribution on the solar cell, and the area which has a larger flux intensity will surely  
459 have a higher temperature or even get hot spots [73]. Coventry et al. [39] found that  
460 the central illuminated region of the cell may be as much as 14°C hotter than the  
461 edges of the cell through the experiment. Furthermore, the reduction of the  
462 illuminated area will cause an increasing temperature gradient. Secondly, each cell  
463 can't be exactly the same, so the differences between them will cause the differences  
464 in their performance and therefore may cause the temperature difference. Finally, in

465 order to avoid the damage of cells caused by the excessive temperature when using  
466 them, every system will have a heat sink. However, even if the solar cell is uniformly  
467 illuminated, temperature non-uniformities are always existed because of the  
468 imperfections in the cell-to-substrate bond, and the temperature gradient may exist  
469 along its diameter because of the properties of the heat sink geometry [74].

470 In all the consequences about the non-uniform temperature, the excessive  
471 temperature is the primary problem. It can bring many harm, and with the increase of  
472 the concentration ratio, this problem will become more obvious [75]. So in the  
473 discussion of the harm, we mainly discuss the efficiency loss caused by the excessive  
474 temperature and the solution to this problem.

475 The effect of temperature can be concluded in two ways: (1) for solar cells, it  
476 may exhibit a short-time degradation due to the local overheating, resulting in loss of  
477 efficiency [76], and it will also cause long-term irreversible damage and reduce the  
478 lifespan rapidly [77] and the PV cells, much like the high-performance CPUs and  
479 GPUs, failures are always instantaneous and catastrophic[78]; (2) for the whole  
480 system, it will affect the system reliability and the whole economic benefits.

## 481 4.2 Cell parameters analysis under non-uniform temperature

### 482 4.2.1 Temperature distribution profile

483 A Gaussian illumination profile has been used as the actual temperature profile  
484 as shown in Fig. 20 [31]. It is assumed that three fourths of the total energy can reach  
485 on the front surface of the cell. And if most heat generation occurs in the central  
486 region of a cell, this region will get the highest operating temperature, so there exists a

487 temperature difference between the center and the outer edge of the cell [31].

488

#### 489 4.2.2 Variation of cell parameters

490 Studies present that the operating temperature is a key factor to influence the  
491 conversion efficiency. The increase in the cell temperature cause a reduction of the  
492 open circuit voltage, which affects the maximum power output delivered by the cell  
493 and leads to the cell efficiency decrease. Tiwari et al. [79] summarized the cell  
494 efficiency changed by the cell temperature during a day. It can be concluded that the  
495 cell efficiency decreases along with the cell temperature increase and at the end of the  
496 day it will again increase due to the decrease in cell temperature (Fig. 21).  
497 Pérez-Higueras et al. [19] also observed that the efficiency of the cell decreased when  
498 the temperature rose using a multi-junction cell (Fig. 22). Skoplaki and Palyvos [80]  
499 indicated that for most of the silicon-based PV cells with the temperature of 25 °C, the  
500 average decrease in efficiency is of the order of 0.45% per degree rise in operating  
501 temperature. Under the concentrating condition, the influence of temperature on the  
502 cells will surely become larger. Since the cell efficiency decreases with increasing  
503 temperature, the cell at the highest temperature will limit the whole string cells  
504 efficiency [29].

505

506 The influence of the temperature of mono-Si solar cells with the p–n junction on  
507 different cell parameters was studied by Meneses-Rodríguez et al. [81]. It can be  
508 found that the open circuit voltage and fill factor  $FF$  have significantly decreased

509 with the increase of temperature while the short-circuit current  $I_{sc}$  has no significant  
510 change (Fig. 23).

511

512 For InGaP/InGaAs/Ge triple-junction solar cells, from Fig. 24, the  $V_{oc}$ ,  $FF$  and  
513  $\eta$  all decreased with the increasing temperature. It can be found that the decline of  
514  $V_{oc}$ ,  $FF$  and  $\eta$  have about 0.5, 0.04 and 0.03 with 140 °C compared to 20 °C at  
515 200 suns. And the  $I_{sc}$  remain almost the same when the concentration ratio is not  
516 much high. Under the concentration ratio at 200 suns, the  $I_{sc}$  has a small increase of  
517 200mA. Therefore the InGaP/InGaAs/Ge triple-junction solar cells have an advantage  
518 over crystalline-silicon solar cells under high-temperature conditions [56].

519

520 Peharz et al. [24] also investigated the temperature impact on different CPV  
521 modules with GaInP/GaInAs/Ge triple-junction solar cells. An indoor sun simulator  
522 was used [82] which was investigated in recent years to control the various  
523 temperature. The  $I-V$  curves and consequences of different parameters (Fig. 25 and  
524 Fig. 26). The open circuit voltages decreases linearly by 0.18%/K of temperature  
525 increase and the  $FF$  shows a relative decrease of 0.16%/K. In contrast, the  $I_{sc}$  is  
526 expected to increase of 0.13%/K with increasing module temperature. It is concluded  
527 that the temperature dependence of Fresnel lenses and thermal expansion of the CPV  
528 modules would reduce the positive short circuit current temperature coefficient of the  
529 solar cells [83]. Siefer et al. [84] did a further study in the same circumstances. The  
530 data shown in Fig. 27 revealed that the energy conversion efficiency  $\eta$ ,  $V_{oc}$  and  $FF$



531 also decreased with the increased temperature. The main reason for the decline is that  
532 the open circuit voltage  $V_{oc}$  will decrease when operated at a high temperature under  
533 concentration.

534

535 The results of the Gaussian temperature profile and an equivalent temperature  
536  $T_0 = 323$  K and a temperature peak  $\Delta T = 20$  K ( $\Delta T$  is the temperature amplitude with  
537 respect to the temperature baseline  $T_0$ ) were shown in Fig. 8 in Section 3.2.2 above.

538 And when the temperature peak  $\Delta T = 40$  K and the equivalent temperature rose to  
539  $T_0 = 334$  K, the decline of  $FF$  is 0.05 and  $V_{oc}$  is 7mV under the Gaussian  
540 temperature situation compared to UT situation from their data (Fig. 28 [45]). Two  
541 conclusions can be gotten from the two results shown respectively: (1) the fill factor  
542  $FF$  and the open circuit voltage  $V_{oc}$  all decrease when the temperature distribution  
543 is more uneven; (2) the fill factor  $FF$  and the open circuit voltage  $V_{oc}$  all decrease  
544 with the increasing temperature.

545

546 And here a comparison of the cell performance between the uniform and  
547 non-uniform temperature is listed in Table 4.

548

#### 549 4.3 Improvement methods

550 For multi-junction solar cells such as the GaInP/GaAs/Ge solar cell, under  
551 concentrated sunlight, about 37% of the absorbed energy is used for generating  
552 electrical power whereas 63% of it is dissipated in heat. Heat dissipation is important

553 because  $V_{oc}$  which is related to the efficiency of solar cells has a negative correlation  
554 with the temperature [21]. So two kinds of methods can be employed to improve this  
555 problem, and one is to control the generation of heat by cells and the other is to use  
556 the cooling system. In the first case, we can reduce the internal resistance of the cell  
557 pack or improve the charging and discharging efficiency of cell under high  
558 temperature. But the inherent chemical heat produced by cell inside can't be avoided,  
559 so just consider for the adjustment of the cell may cannot effectively solve the  
560 problem. Therefore, another case which gains further efficiency is accomplished by a  
561 cooling system to reduce the cell temperature [87] and [88] and the heat dissipated  
562 from the solar cells can be further utilized at the same time where hybrid technologies  
563 were developed for combined heat and power (CHP) cogeneration since the 1970s  
564 [89]. Cooling of photovoltaic cells is paid more attention when designing  
565 concentrating photovoltaic systems. The cooling mechanism should be chosen for the  
566 proper thermal regulation. The type of cooling technology depends upon various  
567 parameters such as the area available for cooling, the fluid flow rate and the heat  
568 transfer coefficient. It needs to follow this principle as follows: the reliability of the  
569 system, the security of starting and running, the cooling efficient and cell temperature  
570 uniformity, whether the system can save energy and the system should meet different  
571 needs [90]. The cooling technology can be divided into passive and active, and the  
572 passive one have advantages of low cost and simple structure. But it is insufficiently  
573 used for LCPV systems and almost cannot be used for commercial. The active system  
574 has a better cooling effect and reliability [91] and for the active cooling, the heat

575 exchanger design can be optimized to obtain uniform temperature distribution [72],  
576 but it is complex and not safe [92]. And the main goal of this section is to introduce  
577 and provide the current work in the field of CPV cooling technology.

#### 578 4.3.1 The traditional cooling methods

579 Traditional cooling methods are mainly consisted of air cooling technology and  
580 water cooling technology.

- 581 ● Air cooling technology

582 Air can take heat away to keep cell's temperature in a low level by convection  
583 passively or actively from the back of the solar cell. Hussain et al. [93] established a  
584 cooling channel under the absorber plate in which the air can flow to take away the  
585 heat. Araki et al. [94] studied the single solar cell cooling problems under 500 X  
586 concentrator, and the results showed that the thermal contact between solar cell and  
587 aluminum plate is also the key to keep its low temperature.

- 588 ● Water cooling technology

589 Water cooling offers a good performance because of its high convection coefficient  
590 and thermal capacity. The key to design is to guarantee the good heat transfer and  
591 electric insulation between the solar cell and the heat exchanger. Verlinden et al. [95]  
592 described an integral water cooling technology using a monolithic silicon concentrator  
593 module consisted of 10 cells (Fig. 29). The module got a 0.8% growth of efficiency  
594 when operated at 25°C compared to 39°C. Verlinden [96] reported an active water  
595 cooling system based on the reflective parabolic dish and set up parallel narrow flow  
596 on the back of the solar cell. The PV receiver is composed of 16 modules, each with

597 24 series-connected silicon solar cells. The cell efficiency can reach 24% and the  
598 system comprehensive energy utilization efficiency can surpass 70%.

599 The advantages and disadvantages of the two kinds of cooling technology are  
600 obvious. The air cooling technology is cheap and safe while the water cooling  
601 technology is complex and expensive but the thermal properties of water make it far  
602 more efficient as a coolant medium than air.

#### 603 4.3.2 The new cooling technology

604 Nowadays, a lot of new cooling technology has risen up and plays an  
605 increasingly important role in the field. They include the heat pipe cooling technology,  
606 the micro-channels technology, the liquid immersion cooling technology, the  
607 impingement jet cooling technology and the phase change material technology, etc.

##### 608 ● Heat pipe cooling technology

609 Heat pipes are common and efficient heat transfer device. One end is stick to the  
610 solar cell and absorb the heat, and another is exposed to cooling environment (Fig. 30)  
611 [97] and [98]. This technology has many advantages, such as the high thermal  
612 conductivity, the good temperature uniformity, the heat flux variability, the reversible  
613 flow direction, the temperature steady characteristics and the good environment  
614 adaptability [90]. Tarabsheh, et al. [99] put forward the pipe line layout for effective  
615 cooling cell method and the cooling pipes beneath each PV string can enhance the  
616 performance of the PV module.

##### 617 ● Micro-channels technology

618 The size of micro-channels are small and can directly cool the millimeter level

619 heat source, but the temperature gradient and the pressure loss is large, so it is needed  
620 to find ways to improve its structure. The work is concentrated on the optimization of  
621 the micro-channel heat sink [100]. Walpole and Missaggia [101] demonstrated an  
622 alternating-channel-flow micro-channel heat sink which can reduce the surface  
623 temperature variations compared to a conventional one with one-directional flow (Fig.  
624 31) [101]. Yang and Zuo [102] presented a novel multi-layer manifold microchannel  
625 cooling system and the experiment results showed that the surface temperature  
626 difference of the CPV cells was below 6.3 °C which also indicated that multi-layer  
627 manifold micro channel had a heat transfer coefficient of 8235.84 W/m<sup>2</sup> K and its  
628 pressure drop was lower than 3 kPa.

629 ● Liquid immersion cooling technology

630 Liquid immersion cooling means that solar cells can be immersed directly into  
631 the circulating liquid and the liquid can take the heat away from both the front and  
632 back surface of the PV string [7]. Liu [103] studied the liquid immersion cooling on  
633 cell modules under moderately intensified illuminations. The temperature distribution  
634 of cell module is fairly uniform within 3 °C under turbulent flow mode.

635 ● Impingement jet cooling technology

636 Impingement jet cooling technology can obtain the low thermal resistance and  
637 has been widely used in many industrial fields [104]. For solar cell cooling, the  
638 impinging jets can extract a large amount of heat due to the very thin thermal  
639 boundary layer that is formed in the stagnation zone directly under the impingement.  
640 Royne et al. [105] explored a jet impingement cooling device for arrays of densely

641 packed PV cells. Combined with a model for cell performance at different  
642 temperatures, it was found that there exists a broad optimal operating region for any  
643 system of photovoltaic cells and cooling device at a given illumination level.

644 ● Phase change material technology

645 PCMs can store the excess heat through melting change in phase and at the  
646 same time it has a constant temperature during the phase change process. Based on  
647 this this feature PV cells can achieve the uniform temperature operation condition.  
648 Researchers have used PCMs in different energy conversion systems, including PV  
649 systems to maintain a high efficiency [106]. Sharma et al. [107] presented an  
650 experimental employing the phase change materials (PCM) to enhance performance  
651 of low-concentration Building-Integrated Concentrated Photovoltaic system via  
652 thermal regulation. The results showed that the relative electrical efficiency can  
653 increase by 7.7% due to PCM incorporation and the module centre temperature has an  
654 average reduction of 3.8 °C compare to the naturally ventilated system without PCM.

655 Here a comparison of the different cooling methods is listed in Table 5.

656

657 **5. Dual effect**

658 In the realistic use of the CPV systems, the most common situation is that the  
659 non-uniform illumination and temperature which have been found to affect the cell  
660 efficiency and overall system performance in a negative way are both existed.  
661 Non-uniform illumination could produce the significant local heating in concentration  
662 solar cells and therefore also cause non-uniform temperature. So the comprehensive

663 effects of them is discussed here.

664 First the effects on cells in the majority situations due to the non-uniformity are  
665 summarized below:

- 666 ● Increase in cell temperature.
- 667 ● Increase in series resistance.
- 668 ● Increase in short circuit current.
- 669 ● Decrease in open circuit voltage.
- 670 ● Decrease in fill factor.
- 671 ● Decrease in efficiency.

672 It is worth mentioning two points in particular. One is that the short circuit  
673 current is hardly affected by non-uniform illumination, but the temperature influence  
674 on it is positive, especially in high concentrator photovoltaic systems [19]. Fernández,  
675 et al. [108] did the research on the performance of lattice-matched and metamorphic  
676 triple junction solar cells under different temperatures and spectral conditions and  
677 they also presented the temperature coefficients of the  $IV$  parameters of different  
678 multi-junction (MJ) cells at different concentration ratios [109] and found that the  
679 incident spectrum during a spectrometric characterization has a significant influence  
680 on  $I_{sc}$  and  $P_{mpp}$  but only marginal on  $V_{oc}$ . Another is there exists a special  
681 circumstance that for organic solar cells, the  $FF$  and  $\eta$  increase under the  
682 localized illumination compared to the uniform one [41]. Maybe people could do  
683 further research of this characteristic and make full use of it. Other kinds of solar cells  
684 could have some other special characteristics which are worth being explored in the

685 future too.

686 Luque et al. [110] established a cell model under inhomogeneous illumination  
687 which takes into account the temperature inhomogeneity (Fig. 32). It is concluded that  
688 the illumination inhomogeneity increased the temperature and the series resistance,  
689 therefore reduced the efficiency. But the strong internal ohmic drops will switch off  
690 all the poorer parts of the solar cell and leave only the outstanding central part of it,  
691 causing the efficiency reduction to be much less of what it might have been expected.  
692 Meneses-Rodríguez et al. [81] studied the simultaneous influence of both the  
693 temperature and the illumination (Fig. 33). It can be found that on the whole, the  
694 efficiency increased with the increase of the illumination and the decrease of the  
695 temperature. So in order to obtain a proper efficiency, it needs to select the proper  
696 combination of illumination and temperature. Franklin and Coventry [31] made a  
697 contrast among the conditions of uniform illumination and temperature, non-uniform  
698 illumination and uniform temperature, and non-uniform illumination and temperature.  
699 It can be found that there is a further reduction of  $V_{oc}$  when the cell is exposed to  
700 non-uniform illumination and temperature. They also pointed out that the cell  
701 efficiency  $\eta$  decreases from 17.3% under uniform illumination and temperature, to  
702 16.8% under non-uniform illumination and uniform temperature, and 16.7% under  
703 non-uniform illumination and temperature. So it can be conclude that for  
704 monocrystalline silicon solar cells, both non-uniform illumination and non-uniform  
705 temperature may have a negative impact on the efficiency of the cell and the effect of  
706 non-uniform illumination is greater.



707 Refer to the analysis by Domenech-Garret [45], it can found that both  
708 non-uniform illumination and non-uniform temperature will decrease the  $FF$  and  
709  $V_{oc}$  of the cell model shown in Fig.7. By comparison, the temperature had a greater  
710 impact on  $FF$  and the illumination played a more important role on  $V_{oc}$ .

711 To compensate for the effects of non-uniform illumination, among the several  
712 improvement methods, the changes for cells have smaller benefits and the cost may be  
713 larger. The design for concentrator can lead to considerable modification which could  
714 provide significantly enhancement on  $FF$  and the cost is much lower. The  
715 concentrator can be improved from the material, the processing technology, the  
716 concentrating way and so on.

717 At the same time, under these negative influence, the cell temperature is  
718 considered to increase a lot, and the solutions to the problem, especially the cooling  
719 methods, are discussed above in Section 4.3. It can be concluded that a reasonable  
720 cooling system design is significant in CPV systems. A good cooling system can not  
721 only reduce cell temperature, but also decrease the negative influence of non-uniform  
722 illumination and cell temperature. Among all the cooling methods, they each have  
723 their own advantages and disadvantages. The traditional cooling methods are more  
724 mature, the air cooling technology is mainly used on single cell and the water cooling  
725 technology is used in LCPV systems which has a better cooling effect. For the new  
726 cooling methods, micro-channels technology and impingement jet cooling technology  
727 are used for HCPV systems for their high heat transfer coefficient. While heat pipe  
728 cooling technology has a wide scope of application and liquid immersion cooling

729 technology can be applied in linear concentrating systems for its good heat-sinking  
730 capability.

731

## 732 **6. Conclusion**

733 In this paper, the performance of concentrator cell under non uniform  
734 illumination and temperature and the improvement methods have been presented. An  
735 overview of concentrating solar cells is introduced. Nowadays, solar cells have a  
736 widely use in CPV systems and have lots of differences with each other. And when  
737 these cells are used to investigate the effect of non-uniformity, models need to be  
738 established by using theoretical and finite element methods in 1-D, 2-D or 3-D.

739 The non-uniform illumination can be caused by the concentrator design, the  
740 improper relative position of the solar cell etc. It displays in two aspects of localized  
741 illumination and the inhomogeneous of the whole cell. And it can lead to an obvious  
742 decrease in open circuit voltage, fill factor and efficiency, especially for  
743 multi-junction solar cells. These problems can be partially solved by changing cell  
744 surface pattern, choosing proper cell material and concentrator. Non-uniform  
745 temperature is mainly caused by the non-uniform illumination, and other factors such  
746 as the arrangement of the cell among a cell pack, and the cooling mechanism etc. The  
747 greatest danger of it is the local excessive temperature which cause decrease in the  
748 open circuit voltage, the fill factor and the efficiency. Particularly, the short circuit  
749 current will increase with the increased temperature, especially in HCPV systems.  
750 People often use different cooling technology to reduce this influence. However, in

751 reality, these two cases are usually co-exist, scientists can search for the influence of  
752 various parameters further by experiments to seek a better solution to reduce the  
753 influence of the non-uniformity.

754

#### 755 **Acknowledgement**

756 The study was sponsored by the National Science Foundation of China (Grant Nos.  
757 51408578, 51476159, 51611130195), Anhui Provincial Natural Science Foundation  
758 (1508085QE96).

759

#### 760 **References**

761 [1] Sahu B K. A study on global solar PV energy developments and policies with  
762 special focus on the top ten solar PV power producing countries. Renewable and  
763 Sustainable Energy Reviews, 2015, 43: 621-634.

764 [2] Liu M, Tay N H S, Bell S, et al. Review on concentrating solar power plants and  
765 new developments in high temperature thermal energy storage technologies.  
766 Renewable and Sustainable Energy Reviews, 2016, 53: 1411-1432.

767 [3] Huang H, Su Y, Gao Y, et al. Design analysis of a Fresnel lens concentrating PV  
768 cell. International Journal of Low-Carbon Technologies, 2011, 6(3): 165-170.

769 [4] Srikanth Madala and Robert F. Boehm. A review of nonimaging solar  
770 concentrators for stationary and passive tracking applications. Renewable and  
771 Sustainable Energy Reviews, 2017, 71: 309-322. Energy Materials and Solar Cells,  
772 2017, 161: 305-327.

773 [5] Würfel P, Würfel U. Physics of solar cells: from basic principles to advanced

- 774 concepts. John Wiley & Sons, 2009.
- 775 [6] Swanson R M. The promise of concentrators. *Progress in Photovoltaics Research*  
776 *and Applications*, 2000, 8(1): 93-111.
- 777 [7] Kurtz S, Geisz J. Multijunction solar cells for conversion of concentrated sunlight  
778 to electricity. *Optics express*, 2010, 18(101): A73-A78.
- 779 [8] Katie Shanks, S. Senthilarasu, Tapas K. Mallick. *Optics for concentrating*  
780 *photovoltaics: Trends, limits and opportunities for materials and design.*  
781 *Renewable and Sustainable Energy Reviews*, 2016, 60: 394-407.
- 782 [9] Jakhar S, Soni M S, Gakkhar N. Historical and recent development of  
783 concentrating photovoltaic cooling technologies. *Renewable and Sustainable*  
784 *Energy Reviews*, 2016, 60: 41-59.
- 785 [10] Xing Ju, Chao Xu, Yangqing Hu, et al. A review on the development of  
786 photovoltaic/concentrated solar power (PV-CSP) hybrid systems. *Solar Energy*  
787 *Materials and Solar Cells*, 2017, 161: 305-327.
- 788 [11] Hosenuzzaman M, Rahim N A, Selvaraj J, et al. Global prospects, progress,  
789 policies, and environmental impact of solar photovoltaic power generation.  
790 *Renewable and Sustainable Energy Reviews*, 2015, 41: 284-297.
- 791 [12] Lee C J, Lin J F. High-efficiency concentrated optical module. *Energy*, 2012,  
792 44(1): 593-603.
- 793 [13] Tyagi V V, Rahim N A A, Rahim N A, et al. Progress in solar PV technology:  
794 Research and achievement. *Renewable and Sustainable Energy Reviews*, 2013,  
795 20: 443-461.

- 796 [14] Green M A. Third generation photovoltaics: solar cells for 2020 and beyond.  
797       Physica E: Low-dimensional Systems and Nanostructures, 2002, 14(1): 65-70.
- 798 [15] Candelise C, Winkler M, Gross R J K. The dynamics of solar PV costs and prices  
799       as a challenge for technology forecasting. Renewable and Sustainable Energy  
800       Reviews, 2013, 26: 96-107.
- 801 [16] Tripathi B, Yadav P, Lokhande M, et al. Feasibility study of commercial silicon  
802       solar PV module based low concentration photovoltaic system. International  
803       Journal of Electrical and Electronics Engineering Research, 2012, 2(3): 84-93.
- 804 [17] Amanlou Y, Hashjin T T, Ghobadian B, et al. A comprehensive review of  
805       Uniform Solar Illumination at Low Concentration Photovoltaic (LCPV) Systems.  
806       Renewable and Sustainable Energy Reviews, 2016, 60: 1430-1441.
- 807 [18] Fernández E F, Almonacid F, Rodrigo P, et al. Calculation of the cell temperature  
808       of a high concentrator photovoltaic (HCPV) module: a study and comparison of  
809       different methods. Solar Energy Materials and Solar Cells, 2014, 121: 144-151.
- 810 [19] Pérez-Higueras P, Muñoz E, Almonacid G, et al. High Concentrator  
811       PhotoVoltaics efficiencies: Present status and forecast. Renewable and  
812       Sustainable Energy Reviews, 2011, 15(4): 1810-1815.
- 813 [20] Rodrigo P, Fernández E F, Almonacid F, et al. Review of methods for the  
814       calculation of cell temperature in high concentration photovoltaic modules for  
815       electrical characterization. Renewable and Sustainable Energy Reviews, 2014, 38:  
816       478-488.
- 817 [21] Kinsey G S, Hebert P, Barbour K E, et al. Concentrator multijunction solar cell

818 characteristics under variable intensity and temperature. Progress in  
819 Photovoltaics: Research and Applications, 2008, 16(6): 503-508.

820 [22] Kinsey G S, Pien P, Hebert P, et al. Operating characteristics of multijunction  
821 solar cells. Solar Energy Materials and Solar Cells, 2009, 93(6): 950-951.

822 [23] Yupeng Xing, Kailiang Zhang, Jinshi Zhao, et al. Thermal and electrical  
823 performance analysis of silicon vertical multi-junction solar cell under  
824 non-uniform illumination. Renewable Energy, 2016, 90: 77-82.

825 [24] Peharz G, Rodríguez J P F, Siefert G, et al. A method for using CPV modules as  
826 temperature sensors and its application to rating procedures. Solar Energy  
827 Materials and Solar Cells, 2011, 95(10): 2734-2744.

828 [25] Araki K, Kondo M, Uozumi H, et al. Achievement of 27% efficient and 200Wp  
829 concentrator module and the technological roadmap toward realization of more  
830 than 31% efficient modules. Solar energy materials and solar cells, 2006, 90(18):  
831 3312-3319.

832 [26] King R R, Law D C, Edmondson K M, et al. 40% efficient metamorphic  
833 GaInP/GaInAs/Ge multijunction solar cells. Applied physics letters, 2007, 90(18):  
834 183516-183900.

835 [27] Guter W, Schöne J, Philipps S P, et al. Current-matched triple-junction solar cell  
836 reaching 41.1% conversion efficiency under concentrated sunlight. Applied  
837 Physics Letters, 2009, 94(22): 223504.

838 [28] Rodrigo P, Fernández E F, Almonacid F, et al. Models for the electrical  
839 characterization of high concentration photovoltaic cells and modules: a review.

840 Renewable and Sustainable Energy Reviews, 2013, 26: 752-760.

841 [29] Algora C, Baudrit M, Rey-Stolle I, et al. Pending issues in the modeling of  
842 concentrator solar cells//19th European Photovoltaic conference, Paris. 2004.

843 [30] Algora C. The importance of the very high concentration in third-generation solar  
844 cells. Next Generation Photovoltaics, 2003: 108-136.

845 [31] Franklin E, Coventry J. Effects of highly non-uniform illumination distribution  
846 on electrical performance of solar cells. 2002.

847 [32] Mellor A, Domenech-Garret J L, Chemisana D, et al. A two-dimensional finite  
848 element model of front surface current flow in cells under non-uniform,  
849 concentrated illumination. Solar Energy, 2009, 83(9): 1459-1465.

850 [33] Galiana B, Algora C, Rey-Stolle I, et al. A 3-D model for concentrator solar cells  
851 based on distributed circuit units. Electron Devices, IEEE Transactions on, 2005,  
852 52(12): 2552-2558.

853 [34] Galiana B, Rey-Stolle I, Algora C, et al. 3D distributed model for concentrator  
854 solar cells//Proceedings of the 19th European Photovoltaic Solar Energy  
855 Conference. 2004, 348.

856 [35] Baig H, Heasman K C, Mallick T K. Non-uniform illumination in concentrating  
857 solar cells. Renewable and Sustainable Energy Reviews, 2012, 16(8):  
858 5890-5909.

859 [36] Segev G, Kribus A. Performance of CPV modules based on vertical  
860 multi-junction cells under non-uniform illumination. Solar Energy, 2013, 88:  
861 120-128.

- 862 [37] Tripanagnostopoulos Y. Linear Fresnel lenses with photovoltaics for cost  
863 effective electricity generation and solar control of buildings//4th International  
864 conference on solar concentrators for the generation of electricity or hydrogen.  
865 El Escorial. 2007.
- 866 [38] Antón I, Sala G. Losses caused by dispersion of optical parameters and  
867 misalignments in PV concentrators. Progress in Photovoltaics: Research and  
868 Applications, 2005, 13(4): 341-352.
- 869 [39] Coventry J S. Performance of a concentrating photovoltaic/thermal solar  
870 collector. Solar Energy, 2005, 78(2): 211-222.
- 871 [40] Coventry J S, Franklin E, Blakers A. Thermal and electrical performance of a  
872 concentrating PV/Thermal collector: results from the ANU CHAPS  
873 collector//ANZSES Solar Energy Conference. Newcastle, Australia, 2002.
- 874 [41] Katz E A, Gordon J M, Tassew W, et al. Photovoltaic characterization of  
875 concentrator solar cells by localized illumination. Journal of Applied Physics,  
876 2006, 100(4): 044514.
- 877 [42] Manor A, Katz E A, Andriessen R, et al. Study of organic photovoltaics by  
878 localized concentrated sunlight: Towards optimization of charge collection in  
879 large-area solar cells. Applied Physics Letters, 2011, 99(17): 173305.
- 880 [43] Johnston G. Focal region measurements of the 20m<sup>2</sup> tiled dish at the Australian  
881 National University. Solar Energy, 1998, 63(2): 117-124.
- 882 [44] Herrero R, Victoria M, Domínguez C, et al. Concentration photovoltaic optical  
883 system irradiance distribution measurements and its effect on multi - junction



884 solar cells. *Progress in Photovoltaics: Research and Applications*, 2012, 20(4):  
885 423-430.

886 [45] Domenech-Garret J L. Cell behaviour under different non-uniform temperature  
887 and radiation combined profiles using a two dimensional finite element model.  
888 *Solar Energy*, 2011, 85(2): 256-264.

889 [46] Algora C. Very-high-concentration challenges of III-V multijunction solar cells.  
890 *Concentrator Photovoltaics*(Springer Series in Optical Sciences Volume 130),  
891 2007, 130: 89-111.

892 [47] Goma S, Yoshioka K, Saitoh T. Effect of concentration distribution on cell  
893 performance for low-concentrators with a three-dimensional lens. *Solar Energy*  
894 *Materials and solar cells*, 1997, 47(1): 339-344.

895 [48] Araki K, Yamaguchi M. Extended distributed model for analysis of non-ideal  
896 concentration operation. *Solar energy materials and solar cells*, 2003, 75(3):  
897 467-473.

898 [49] Sater B, Perales M, Jackson J, et al. Cost-effective high intensity concentrated  
899 photovoltaic system//*Energytech*, 2011 IEEE. IEEE, 2011: 1-6.

900 [50] Pozner R, Segev G, Sarfaty R, et al. Vertical junction Si cells for concentrating  
901 photovoltaics. *Progress in Photovoltaics: Research and Applications*, 2012, 20(2):  
902 197-208.

903 [51] Dolara A, Lazaroiu G C, Leva S, et al. Experimental investigation of partial  
904 shading scenarios on PV (photovoltaic) modules[J]. *Energy*, 2013, 55: 466-475.

905 [52] Wang Y, Pei G, Zhang L. Effects of frame shadow on the PV character of a

- 906 photovoltaic/thermal system[J]. *Applied Energy*, 2014, 130: 326-32.
- 907 [53] Baishali Talukdar, Sukanya Buragohain, Sanjai Kumar, et al. Effect of spectral  
908 response of solar cells on the module output when individually cells are shaded.  
909 *Solar Energy*, 2016, 137: 303-307.
- 910 [54] Silva A R, Miyoshi J, Diniz J A, et al. The Surface Texturing of Monocrystalline  
911 Silicon with NH<sub>4</sub> OH and Ion Implantation for Applications in Solar Cells  
912 Compatible with CMOS Technology. *Energy Procedia*, 2014, 44: 132-137.
- 913 [55] Vivar M, Morilla C, Antón I, et al. Laser grooved buried contact cells optimised  
914 for linear concentration systems. *Solar Energy Materials and Solar Cells*, 2010,  
915 94(2): 187-193.
- 916 [56] Nishioka K, Takamoto T, Agui T, et al. Annual output estimation of concentrator  
917 photovoltaic systems using high-efficiency InGaP/InGaAs/Ge triple-junction  
918 solar cells based on experimental solar cell's characteristics and field-test  
919 meteorological data. *Solar Energy Materials and Solar Cells*, 2006, 90(1): 57-67.
- 920 [57] Or A B, Appelbaum J. Performance analysis of concentrator photovoltaic  
921 dense-arrays under non-uniform irradiance. *Solar Energy Materials and Solar  
922 Cells*, 2013, 117: 110-119.
- 923 [58] Schultz R D, Vorster F J, van Dyk E E. Performance of multi-junction cells due  
924 to illumination distribution across the cell surface. *Physica B: Condensed Matter*,  
925 2012, 407(10): 1649-1652.
- 926 [59] Yoon J, Li L, Semichaevsky A V, et al. Flexible concentrator photovoltaics based  
927 on microscale silicon solar cells embedded in luminescent waveguides. *Nature*

- 928           communications, 2011, 2: 343.
- 929   [60] Zhang J, Wang M, Zhang Y, et al. Optimization of large-size glass laminated  
930           luminescent solar concentrators. *Solar Energy*, 2015, 117: 260-267.
- 931   [61] Xing Y, Han P, Wang S, et al. A review of concentrator silicon solar cells.  
932           *Renewable and Sustainable Energy Reviews*, 2015, 51: 1697-1708.
- 933   [62] Kurtz S R, O'Neill M J. Estimating and controlling chromatic aberration losses  
934           for two-junction, two-terminal devices in refractive concentrator  
935           systems//Photovoltaic Specialists Conference, 1996., Conference Record of the  
936           Twenty Fifth IEEE. IEEE, 1996: 361-364.
- 937   [63] Hatwaambo S, Hakansson H, Roos A, et al. Mitigating the non-uniform  
938           illumination in low concentrating CPCs using structured reflectors. *Solar  
939           Energy Materials and Solar Cells*, 2009, 93(11): 2020-2024.
- 940   [64] Ricardo Perez-Enciso, Alessandro Gallo, David Riveros-Rosas, et al. A simple  
941           method to achieve a uniform flux distribution in a multi-faceted point focus  
942           concentrator. *Renewable Energy*, 2016, 93: 115-124.
- 943   [65] Naichia Yeh. Illumination uniformity issue explored via two-stage solar  
944           concentrator system based on Fresnel lens and compound flat concentrator.  
945           *Energy*, 2016, 95: 542-549.
- 946   [66] Guiqiang L, Gang P, Yuehong S, et al. Experiment and simulation study on the  
947           flux distribution of lens-walled compound parabolic concentrator compared with  
948           mirror compound parabolic concentrator. *Energy*, 2013, 58: 398-403.
- 949   [67] Guiqiang L, Gang P, Jie J, et al. Outdoor overall performance of a novel

- 950 air-gap-lens-walled compound parabolic concentrator (ALCPC) incorporated  
951 with photovoltaic/thermal system. *Applied Energy*, 2015,144: 214-233.
- 952 [68] Guiqiang L, Gang P, Yuehong S, et al. Optical evaluation of a novel static  
953 incorporated compound parabolic concentrator with photovoltaic/thermal system  
954 and preliminary experiment. *Energy Conversion and Management*, 2014, 85:  
955 204-211.
- 956 [69] Guiqiang L, Gang P, Jie J, et al. Structure optimization and annual performance  
957 analysis of the lens-walled compound parabolic concentrator. *International  
958 Journal of Green Energy*, 2016, 13: 944-950.
- 959 [70] Guiqiang L, Gang P, Yuehong S, et al. Design and investigation of a novel  
960 lens-walled compound parabolic concentrator with air gap. *Applied Energy*, 2014,  
961 125: 21-27.
- 962 [71] Guiqiang L, Yuehong S, Gang P, et al. Preliminary Experimental Comparison of  
963 the Performance of a Novel Lens-Walled Compound Parabolic Concentrator  
964 (CPC) with the Conventional Mirror and Solid CPCs. *International Journal of  
965 Green Energy*, 2012, 10: 848-859.
- 966 [72] Bahaidarah H M S, Baloch A A B, Gandhidasan P. Uniform cooling of  
967 photovoltaic panels: A review. *Renewable and Sustainable Energy Reviews*,  
968 2016, 57: 1520-1544.
- 969 [73] Li G, Pei G, Ji J, et al. Numerical and experimental study on a PV/T system with  
970 static miniature solar concentrator. *Solar Energy*, 2015, 120: 565-574.
- 971 [74] Mathur R K, Mehrotra D R, Mittal S, et al. Thermal non-uniformities in

- 972 concentrator solar cells. *Solar cells*, 1984, 11(2): 175-188.
- 973 [75] Jakhar S, Soni M S, Gakkhar N. Historical and recent development of  
974 concentrating photovoltaic cooling technologies. *Renewable and Sustainable  
975 Energy Reviews*, 2016, 60: 41-59.
- 976 [76] Do K H, Kim T H, Han Y S, et al. General correlation of a natural convective  
977 heat sink with plate-fins for high concentrating photovoltaic module cooling.  
978 *Solar Energy*, 2012, 86(9): 2725-2734.
- 979 [77] Sangani C S, Solanki C S. Experimental evaluation of V-trough (2 suns) PV  
980 concentrator system using commercial PV modules. *Solar energy materials and  
981 solar cells*, 2007, 91(6): 453-459.
- 982 [78] Lee S. Thermal challenges and opportunities in concentrated  
983 photovoltaics//*Electronics Packaging Technology Conference (EPTC)*, 2010 12th.  
984 *IEEE*, 2010: 608-613.
- 985 [79] Tiwari G N, Mishra R K, Solanki S C. Photovoltaic modules and their  
986 applications: a review on thermal modelling. *Applied Energy*, 2011, 88(7):  
987 2287-2304.
- 988 [80] Skoplaki E, Palyvos J A. Operating temperature of photovoltaic modules: A  
989 survey of pertinent correlations. *Renewable Energy*, 2009, 34(1): 23-29.
- 990 [81] Meneses-Rodríguez D, Horley P P, Gonzalez-Hernandez J, et al. Photovoltaic  
991 solar cells performance at elevated temperatures. *Solar energy*, 2005, 78(2):  
992 243-250.
- 993 [82] Domínguez C, Antón I, Sala G. Solar simulator for concentrator photovoltaic

994 systems. Optics express, 2008, 16(19): 14894-14901.

995 [83] Schult T, Neubauer M, Bessler Y, et al. Temperature dependence of Fresnel  
996 lenses for concentrating photovoltaics//2nd International Workshop on  
997 Concentrating Photovoltaic Optics and Power, Germany. 2009.

998 [84] Siefer G, Bett A W. Analysis of temperature coefficients for III–V  
999 multi - junction concentrator cells. Progress in Photovoltaics: Research and  
1000 Applications, 2014, 22(5): 515-524.

1001 [85] Meneses-Rodríguez D, Horley P P, Gonzalez-Hernandez J, et al. Photovoltaic  
1002 solar cells performance at elevated temperatures. Solar energy, 2005, 78(2):  
1003 243-250.Kerzmann T, Schaefer L. System simulation of a linear concentrating  
1004 photovoltaic system with an active cooling system. Renewable Energy, 2012, 41:  
1005 254-261.

1006 [86] Peharz G, Ferrer Rodríguez J P, Siefer G, et al. Investigations on the temperature  
1007 dependence of CPV modules equipped with triple - junction solar cells. Progress  
1008 in Photovoltaics: Research and Applications, 2011, 19(1): 54-60.

1009 [87] Kerzmann T, Schaefer L. System simulation of a linear concentrating  
1010 photovoltaic system with an active cooling system. Renewable Energy, 2012, 41:  
1011 254-261.

1012 [88] Faiman D. Large-area concentrators//Conference record, Second Workshop on  
1013 The Path to Ultrahigh Efficiency Photovoltaics, JRC Ispra, Italy. 2002.

1014 [89]Xing Ju, Chao Xu, Xue Han, et al. A review of the concentrated  
1015 photovoltaic/thermal (CPVT) hybrid solar systems based on the spectral beam

- 1016 splitting technology. *Applied Energy*, 2017, 187: 534-563.
- 1017 [90] Zhangbo Y, Qifen L, Qunzhi Z, et al. The cooling technology of solar cells under  
1018 concentrated system//Power Electronics and Motion Control Conference, 2009.  
1019 IPEMC'09. IEEE 6th International. IEEE, 2009: 2193-2197.
- 1020 [91] Royne A, Dey C J, Mills D R. Cooling of photovoltaic cells under concentrated  
1021 illumination: a critical review. *Solar energy materials and solar cells*, 2005, 86(4):  
1022 451-483.]
- 1023 [92] Yeom J, Shannon M A, Yogesh G, et al. Micro-coolers//Comprehensive  
1024 Microsystems. Elsevier London, 2008, 3: 499-550.
- 1025 [93] Hussain S, Harrison S J. Experimental and numerical investigations of passive air  
1026 cooling of a residential flat-plate solar collector under stagnation conditions.  
1027 *Solar Energy*, 2015, 122: 1023-1036.
- 1028 [94] Araki K, Uozumi H, Yamaguchi M. A simple passive cooling structure and its  
1029 heat analysis for 500 X concentrator PV module//Conference Record IEEE  
1030 photovoltaic specialists conference. IEEE, 2002, 29(1): 1568-1571.
- 1031 [95] Verlinden P, Sinton R A, Swanson R M, et al. Single-wafer integrated 140 W  
1032 silicon concentrator module//Photovoltaic Specialists Conference, 1991.,  
1033 Conference Record of the Twenty Second IEEE. IEEE, 1991: 739-743.
- 1034 [96] Verlinden P J, Terao A, Smith D D, et al. Will we have a 20%-efficient (PTC)  
1035 photovoltaic system//Proceedings of the 17th european photovoltaic solar energy  
1036 conference. 2001: 385-90.
- 1037 [97] Reay D, McGlen R, Kew P. Heat pipes: theory, design and applications.

- 1038 Butterworth-Heinemann, 2013.
- 1039 [98] Faghri A. Heat pipe science and technology. Global Digital Press, 1995.
- 1040 [99] Al Tarabsheh A, Voutetakish S, Papadopoulosb A I, et al. Investigation of  
1041 Temperature Effects in Efficiency Improvement of Non-Uniformly Cooled  
1042 Photovoltaic Cells. CHEMICAL ENGINEERING, 2013, 35.
- 1043 [100] Chong S H, Ooi K T, Wong T N. Optimisation of single and double layer  
1044 counter flow microchannel heat sinks. Applied Thermal Engineering, 2002,  
1045 22(14): 1569-1585.
- 1046 [101] Walpole J N, Missaggia L J. Microchannel heat sink with alternating flow  
1047 directions: U.S. Patent 5,099,910. 1992-3-31.
- 1048 [102] Kaijun Yang, Chuncheng Zuo. A novel multi-layer manifold microchannel  
1049 cooling system for concentrating photovoltaic cells. Energy Conversion and  
1050 Management, 2015, 89: 214-221
- 1051 [103] Liu L, Zhu L, Wang Y, et al. Heat dissipation performance of silicon solar cells  
1052 by direct dielectric liquid immersion under intensified illuminations. Solar  
1053 Energy, 2011, 85(5): 922-930.
- 1054 [104] Babic D, Murray D B, Torrance A A. Mist jet cooling of grinding processes.  
1055 International Journal of Machine Tools and Manufacture, 2005, 45(10):  
1056 1171-1177.
- 1057 [105] Royne A, Dey C J. Design of a jet impingement cooling device for densely  
1058 packed PV cells under high concentration. Solar energy, 2007, 81(8): 1014-1024.
- 1059 [106] Hasan A, McCormack S J, Huang M J, et al. Evaluation of phase change



1060 materials for thermal regulation enhancement of building integrated  
1061 photovoltaics. *Solar Energy*, 2010, 84(9): 1601-1612.

1062 [107] Shivangi Sharma, Asif Tahir, K.S. Reddy, Tapas K. Mallick. Performance  
1063 enhancement of a Building-Integrated Concentrating Photovoltaic system using phase  
1064 change material. *Solar Energy Materials & Solar Cells*, 2016, 149: 29–39.

1065 [108] Fernández E F, Loureiro A J G, Higuera P J P, et al. Monolithic III-V  
1066 triple-junction solar cells under different temperatures and spectra//*Electron*  
1067 *Devices (CDE)*, 2011 Spanish Conference on. IEEE, 2011: 1-4.

1068 [109] Fernández E F, Siefer G, Schachtner M, et al. Temperature coefficients of  
1069 monolithic III-V triple-junction solar cells under different spectra and irradiance  
1070 levels//*American Institute of Physics Conference Series*. 2012, 1477: 189-193.

1071 [110] Luque A, Sala G, Arboiro J C. Electric and thermal model for non-uniformly  
1072 illuminated concentration cells. *Solar Energy Materials and Solar Cells*, 1998,  
1073 51(3): 269-290.

1074

1075 **Figure captions**

1076 Fig.1.  $I-V$  curves for uniform and non-uniform illumination of a solar cell

1077 Fig.2. A comparison between the key parameters of uniformly and localized  
1078 illuminated cells: (a)  $I_{sc}$ , (b)  $V_{oc}$ , (c)  $FF$ , and (d)  $PCE(\eta)$

1079 Fig.3. Rough illumination profile related to a Gaussian distribution

1080 Fig.4. Simulated  $I-V$  Curves: average concentration ratio = 22.7, average  
1081 temperature = 69°C

1082 Fig.5. Open circuit voltage and efficiency variation with peak illumination intensity

1083 Fig.6. (a) Fill factors and (b) cell efficiencies of cells simulated under Gaussian  
1084 illumination profiles

1085 Fig.7. Open circuit voltage of cells simulated under Gaussian illumination profiles

1086 Fig.8. Sketch of the cell element used in the model

1087 Fig.9. Comparison of the  $I-V$  curves of a cell under three conditions

1088 Fig.10.  $I-V$  curves related to multi-junction (MJ) solar cell under uniform and  
1089 non-uniform illumination

1090 Fig.11.  $FF$  under uniform and non-uniform conditions depend on incident light  
1091 intensity

1092 Fig.12. Calculated  $I-V$  curves under non-uniform flux. The solid lines correspond  
1093 Gaussian-distributed flux density. The dotted lines correspond uniform flux

1094 Fig.13. Shading scenarios: (a) Vertical shading; (b) Horizontal shading; (c) Diagonal  
1095 shading

1096 Fig.14. (a) current-voltage curve and (b) power-voltage curve of poly-crystalline PV

1097 module under horizontally shading process

1098 Fig.15. Circuit diagrams

1099 Fig.16. LGBC technology structure of solar cell

1100 Fig.17. Influences of synthesized chromatic aberration of 3-junction solar cell

1101 Fig.18. (a) Structure of mirror CPC, (b) Structure of lens-walled CPC

1102 Fig.19. Structure of lens-walled CPC with air gap

1103 Fig.20. An example of cell temperature profile depend on cell position

1104 Fig.21. Cell temperature and cell efficiency for a typical day of summer

1105 Fig.22. Differences in the efficiency under various temperature of the multi-junction

1106 cell

1107 Fig.23. The performance of (a)  $I-V$  curves, (b) cell parameters under different

1108 temperatures

1109 Fig.24. The relationship of temperature and (a)  $V_{oc}$  (b)  $I_{sc}$  (c)  $FF$  (d) conversion

1110 efficiency  $\eta$  of InGaP/InGaAs/Ge triple-junction solar cells

1111 Fig.25. The  $I-V$  curves of the investigated modules

1112 Fig.26. The module's electrical parameters dependent on temperature

1113 Fig.27. Open circuit voltage  $V_{oc}$ , fill factor  $FF$  and efficiency  $\eta$  of the

1114  $\text{Ga}_{0.50}\text{In}_{0.50}\text{P}/\text{Ga}_{0.99}\text{In}_{0.01}\text{As}/\text{Ge}$  triple-junction cell at different temperatures

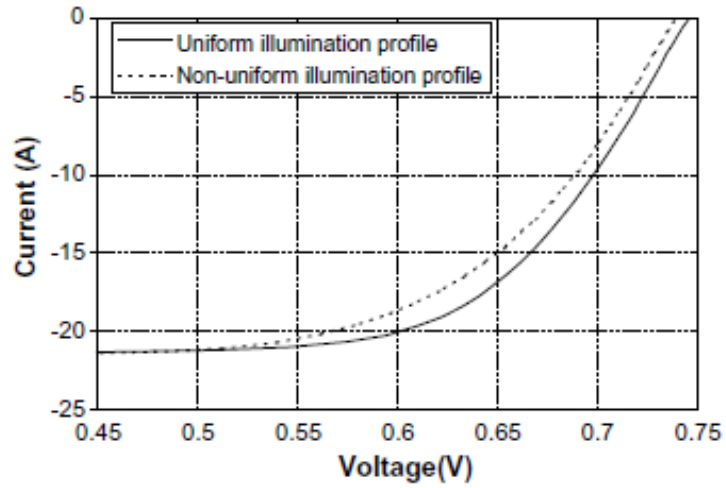
1115 Fig.28. Comparison of the  $I-V$  curves of a cell under three conditions

1116 Fig.29. Cooling structure of the PV module

1117 Fig.30. Heat pipe based cooling system

1118 Fig.31. A cross-sectional view of a portion of the microchannel heat sink

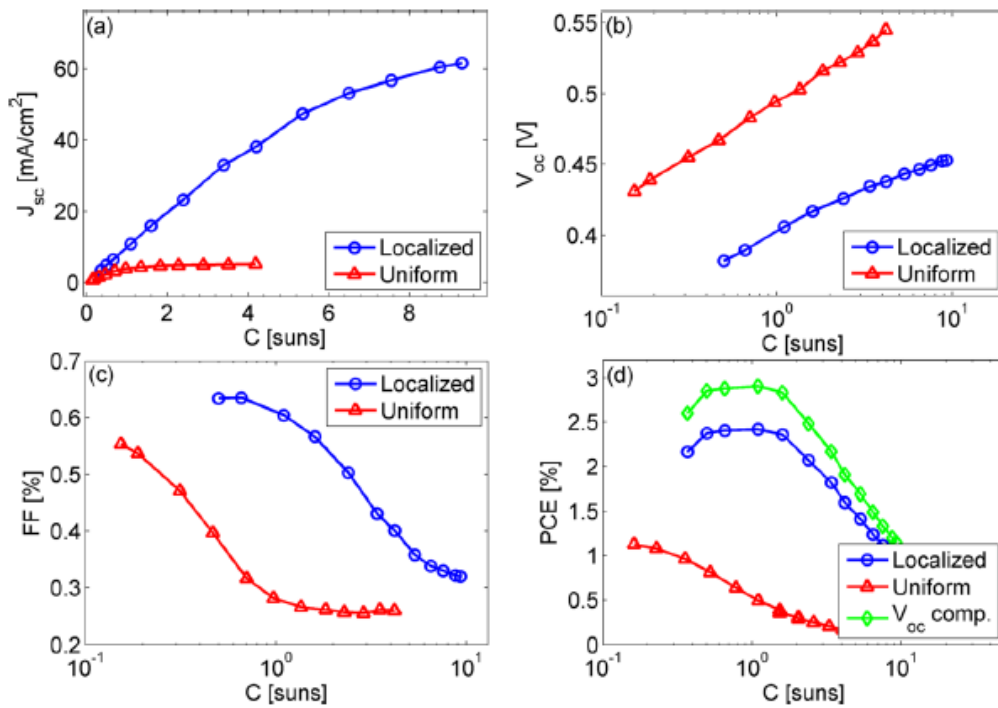
- 1119 Fig.32. Schematic of the cell grid for series resistance calculations
- 1120 Fig.33. Efficiency of solar cells under simultaneous influence of temperature and  
1121 solar concentration
- 1122
- 1123 **Table captions**
- 1124 Table 1.The causes of non-uniform illumination
- 1125 Table2. Cell parameters under 12 suns uniform illumination
- 1126 Table 3. Comparison between uniform and non-uniform illumination.
- 1127 Table 4. Comparison between uniform and non-uniform temperature.
- 1128 Table 5. Comparison of different cooling methods.



1129

1130 Fig.1.  $I-V$  curves for uniform and non-uniform illumination of a solar cell [40].

1131

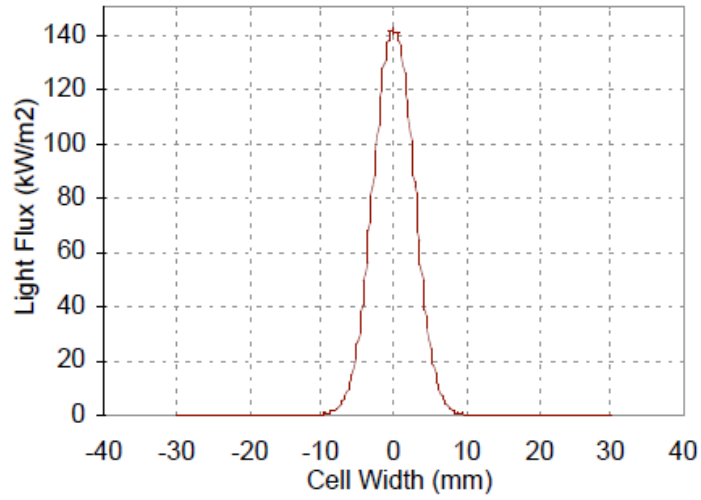


1132

1133 Fig.2. A comparison between the key parameters of uniformly and localized

1134 illuminated cells: (a)  $I_{sc}$ , (b)  $V_{oc}$ , (c)  $FF$ , and (d)  $PCE(\eta)$  [42].

1135

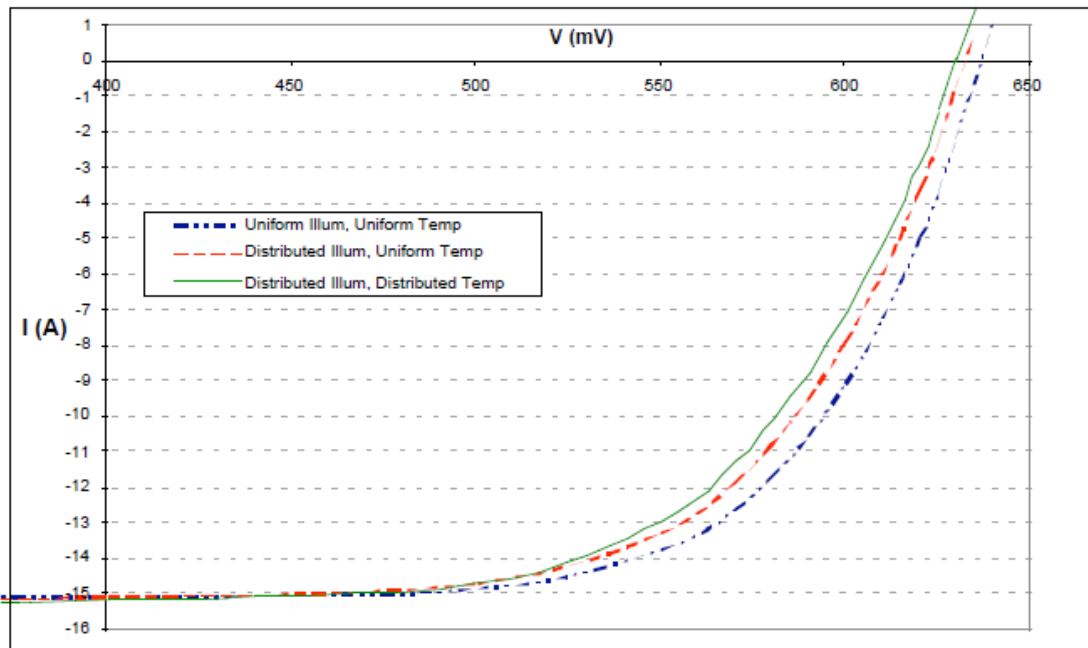


1136

1137

Fig.3. Rough illumination profile related to a Gaussian distribution [45].

1138



1139

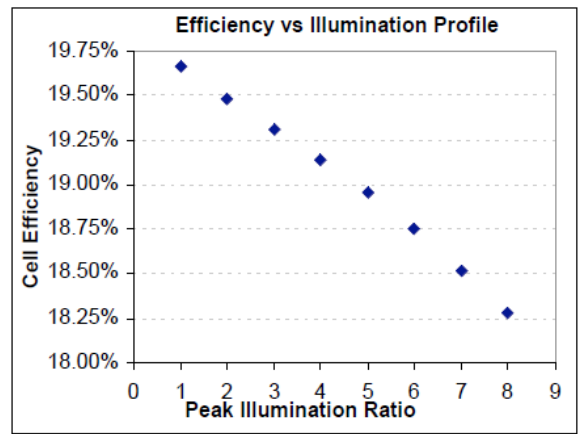
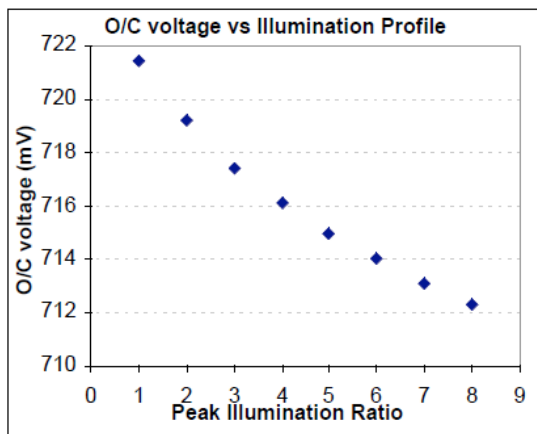
1140

Fig.4. Simulated  $I-V$  Curves: average concentration ratio = 22.7, average

1141

temperature = 69°C [31].

1142



1143

1144 Fig.5. Open circuit voltage and efficiency variation with peak illumination intensity

1145

[31].

1146

1147

1148

1149

1150

1151

1152

1153

1154

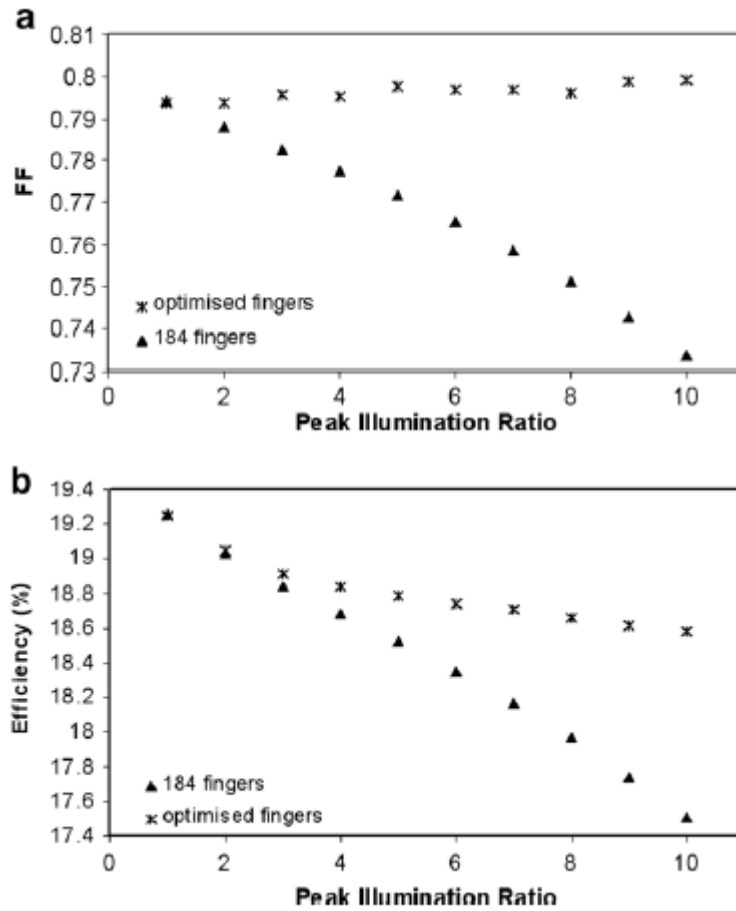
1155

1156

1157

1158

1159



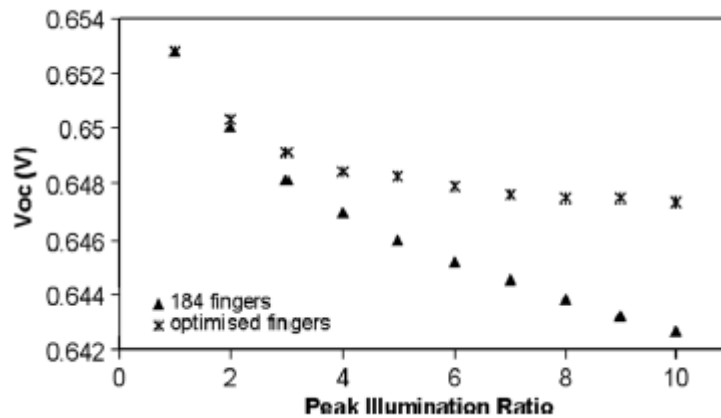
1160

1161

Fig.6. (a) Fill factors and (b) cell efficiencies of cells simulated under Gaussian illumination profiles [32].

1162

1163



1164

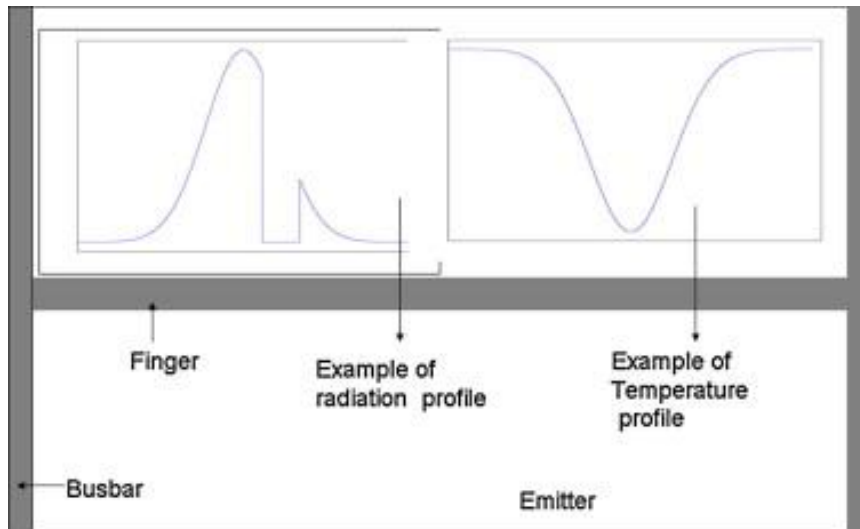
1165

Fig.7. Open circuit voltage of cells simulated under Gaussian illumination profiles

1166

[32]



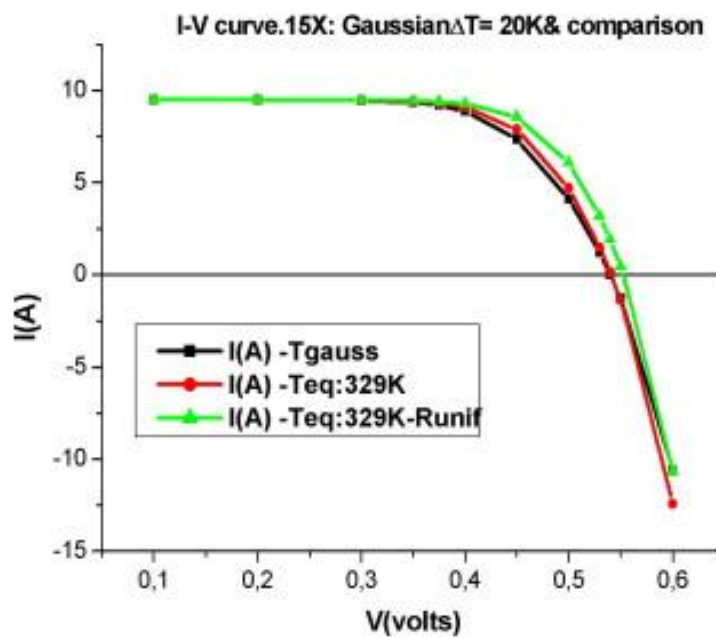


1167

1168

Fig.8. Sketch of the cell element used in the model [32].

1169



1170

1171

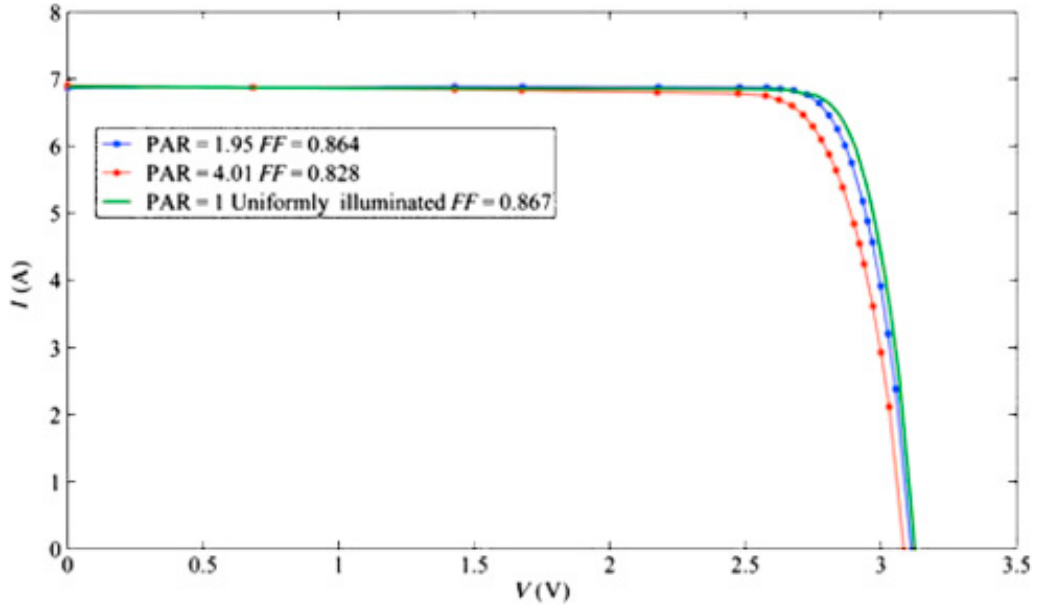
Fig.9. Comparison of the  $I-V$  curves of a cell under three conditions [45].

1172

1173

1174

1175



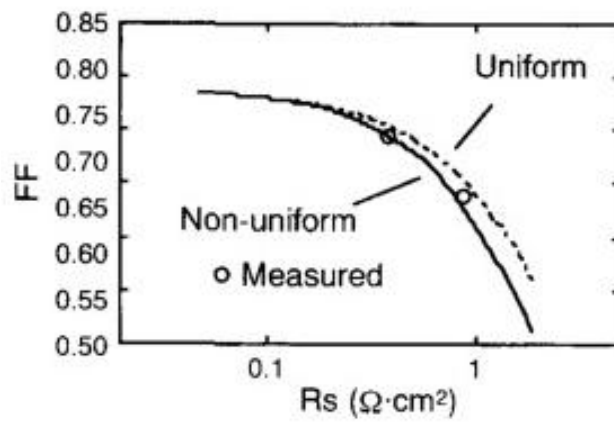
1176

1177 Fig.10.  $I-V$  curves related to multi-junction (MJ) solar cell under uniform and

1178

non-uniform illumination [44].

1179



1180

1181 Fig.11.  $FF$  under uniform and non-uniform conditions depend on incident light

1182

intensity [47].

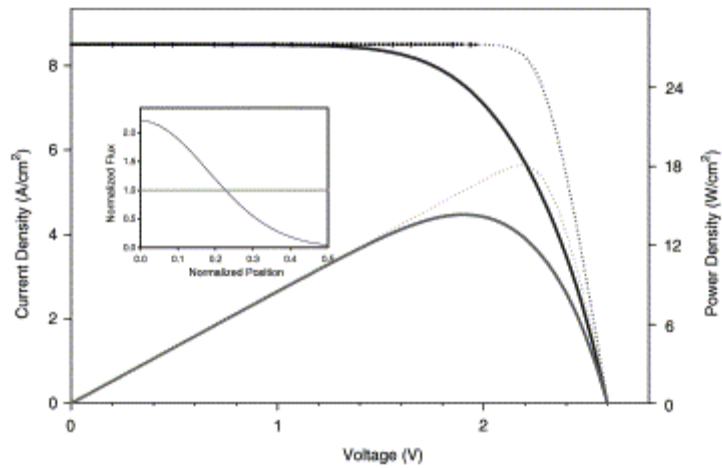
1183

1184

1185

1186

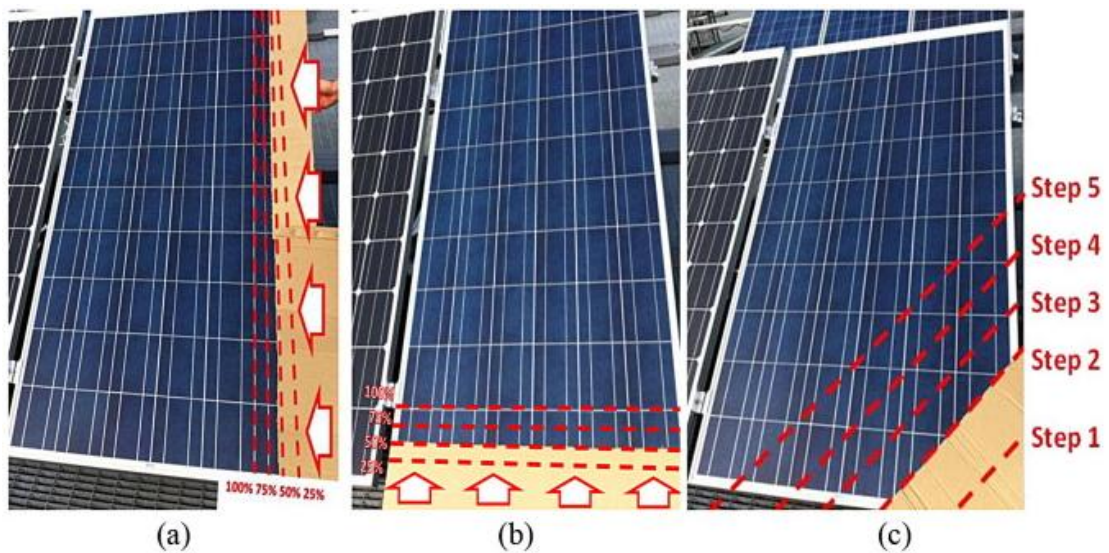
1187



1188

1189 Fig.12. Calculated  $I-V$  curves under non-uniform flux. The solid lines correspond

1190 Gaussian-distributed flux density. The dotted lines correspond uniform flux [48].



1191

1192 Fig.13. Shading scenarios: (a) Vertical shading; (b) Horizontal shading; (c) Diagonal

1193

shading [51].

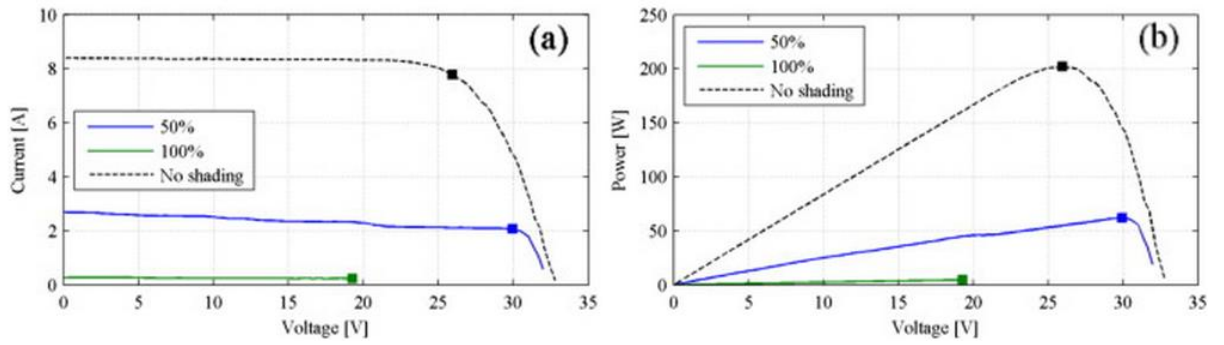
1194

1195

1196

1197

1198

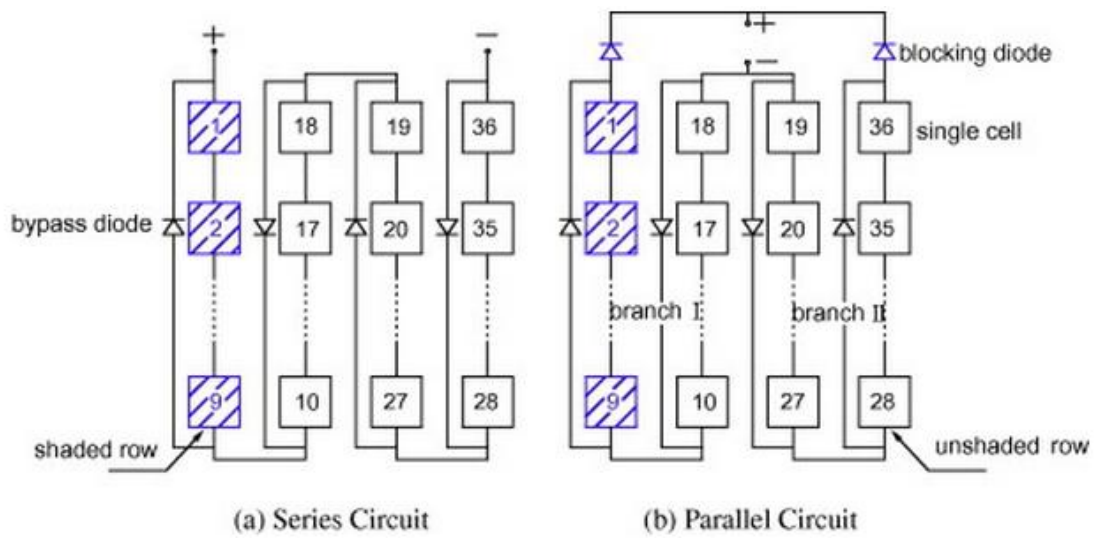


1199

1200 Fig.14. (a) current–voltage curve and (b) power–voltage curve of poly-crystalline PV

1201

module under horizontally shading process [51].

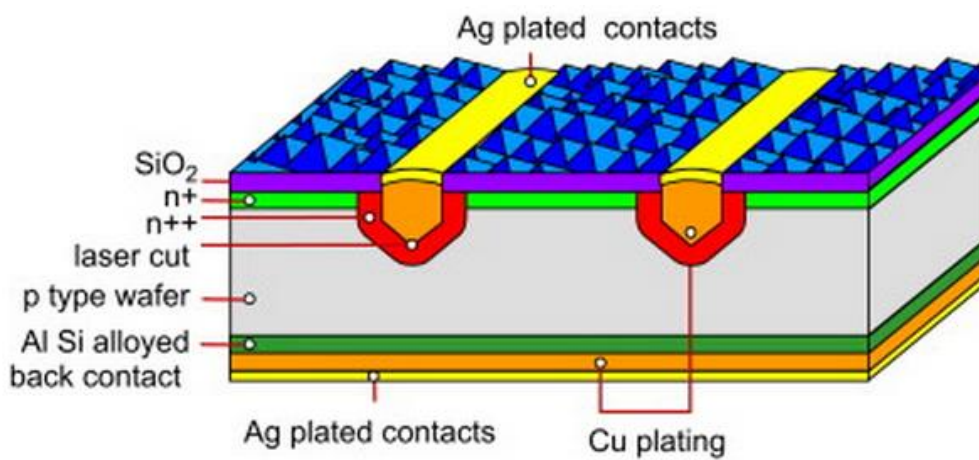


1202

1203

Fig.15. Circuit diagrams [52].

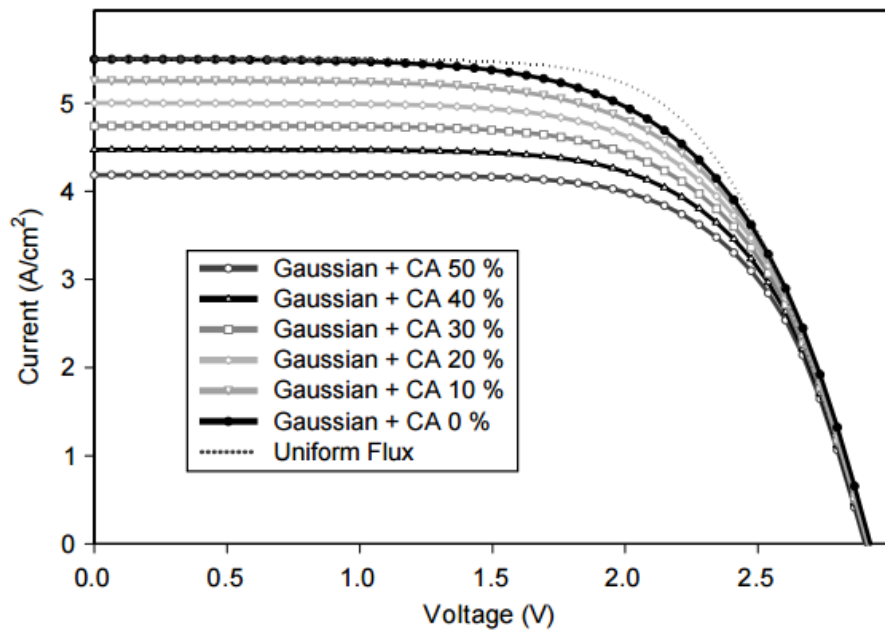
1204



1205

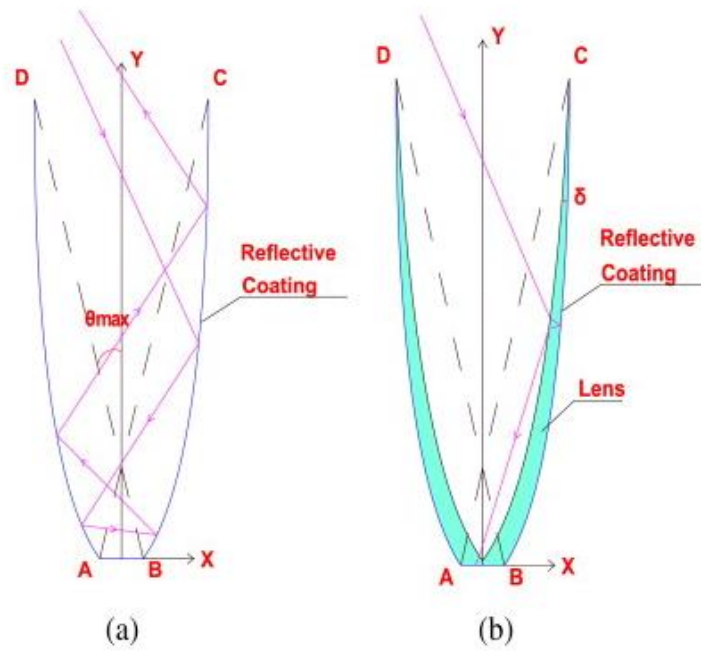
1206

Fig.16. LGBC technology structure of solar cell [54].



1207

1208 Fig.17. Influences of synthesized chromatic aberration of 3-junction solar cell [48].



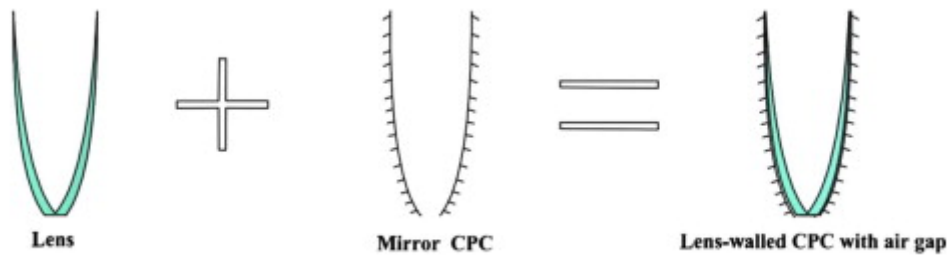
1209

1210 Fig.18. (a) Structure of mirror CPC, (b) Structure of lens-walled CPC [66].

1211

1212

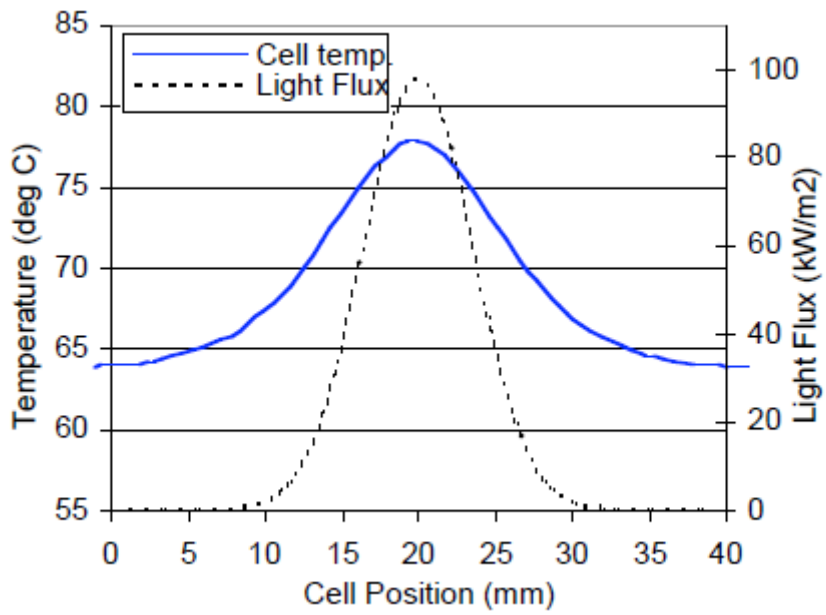
1213



1214

1215

Fig.19. Structure of lens-walled CPC with air gap [70].



1216

1217

Fig.20. An example of cell temperature profile depend on cell position [31].

1218

1219

1220

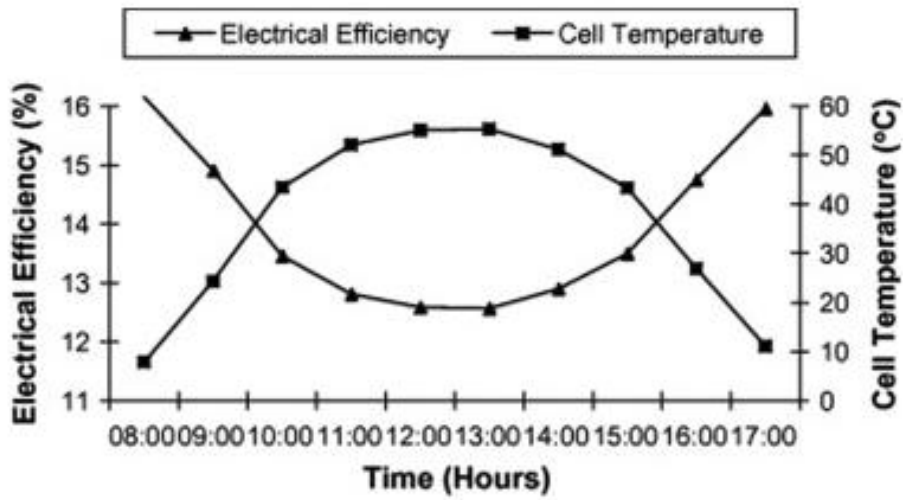
1221

1222

1223

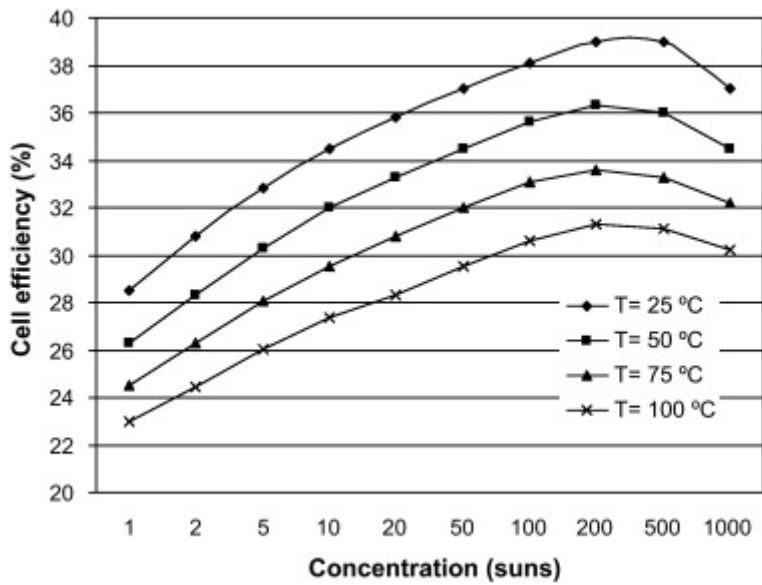
1224

1225



1226

1227 Fig.21. Cell temperature and cell efficiency for a typical day of summer [79].



1228

1229 Fig.22. Differences in the efficiency under various temperature of the multi-junction

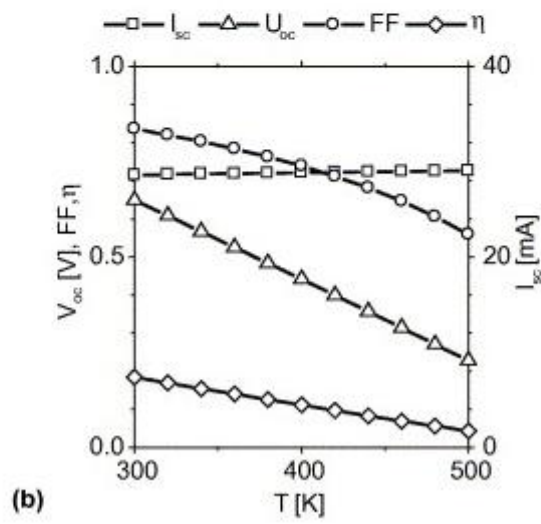
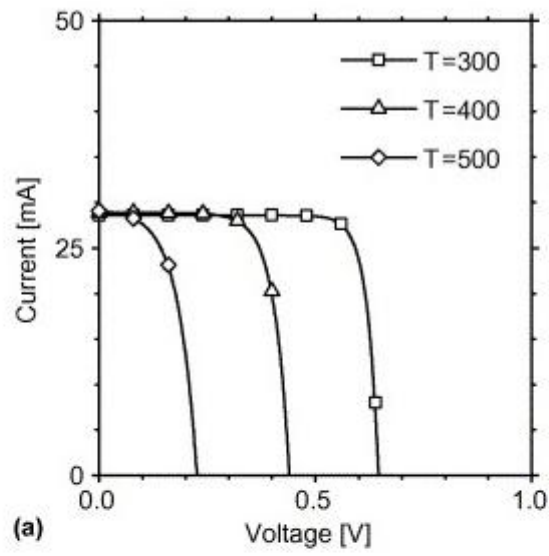
1230

cell [19].

1231

1232

1233



1234

1235 Fig.23. The performance of (a)  $I-V$  curves, (b) cell parameters under different

1236

temperatures [81].

1237

1238

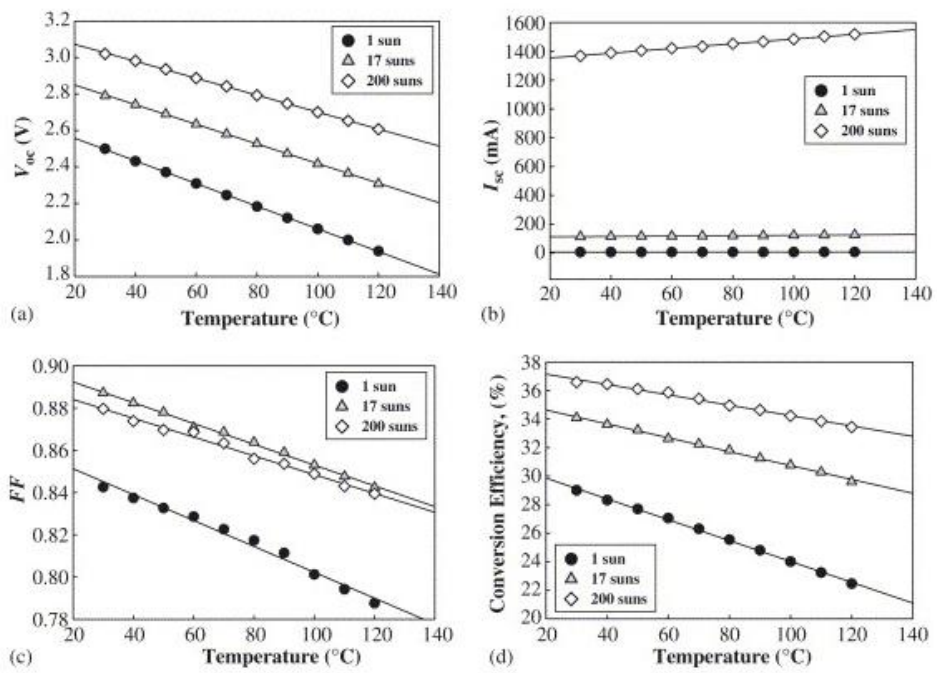
1239

1240

1241

1242

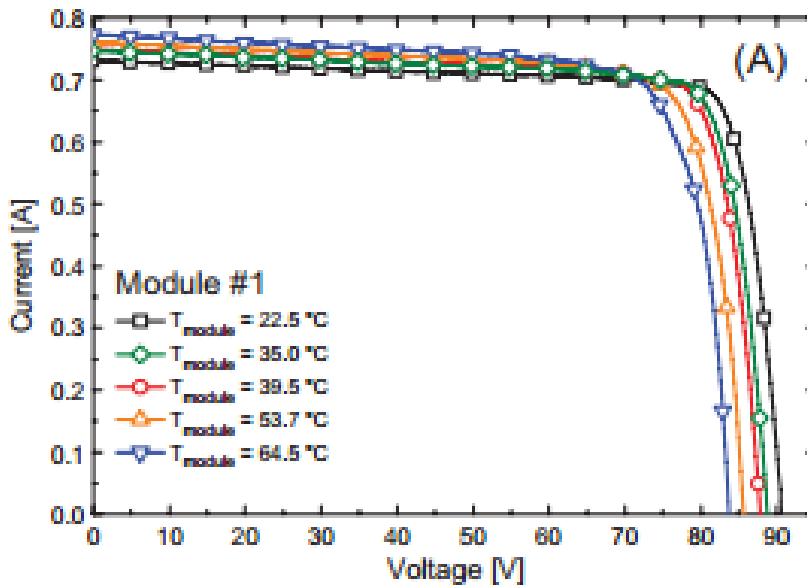




1243

1244 Fig.24. The relationship of temperature and (a)  $V_{oc}$  (b)  $I_{sc}$  (c)  $FF$  (d) conversion

1245 efficiency  $\eta$  of InGaP/InGaAs/Ge triple-junction solar cells [56].

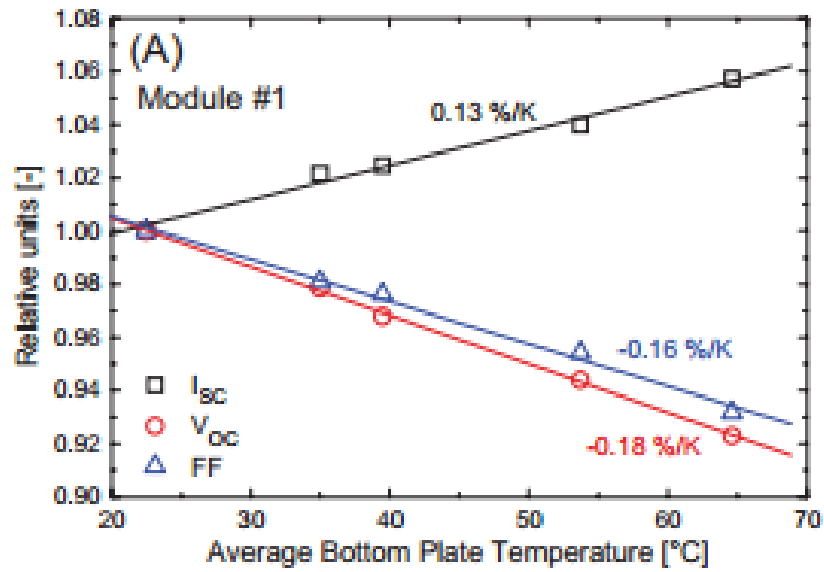


1246

1247 Fig.25. The  $I-V$  curves of the investigated modules [82].

1248

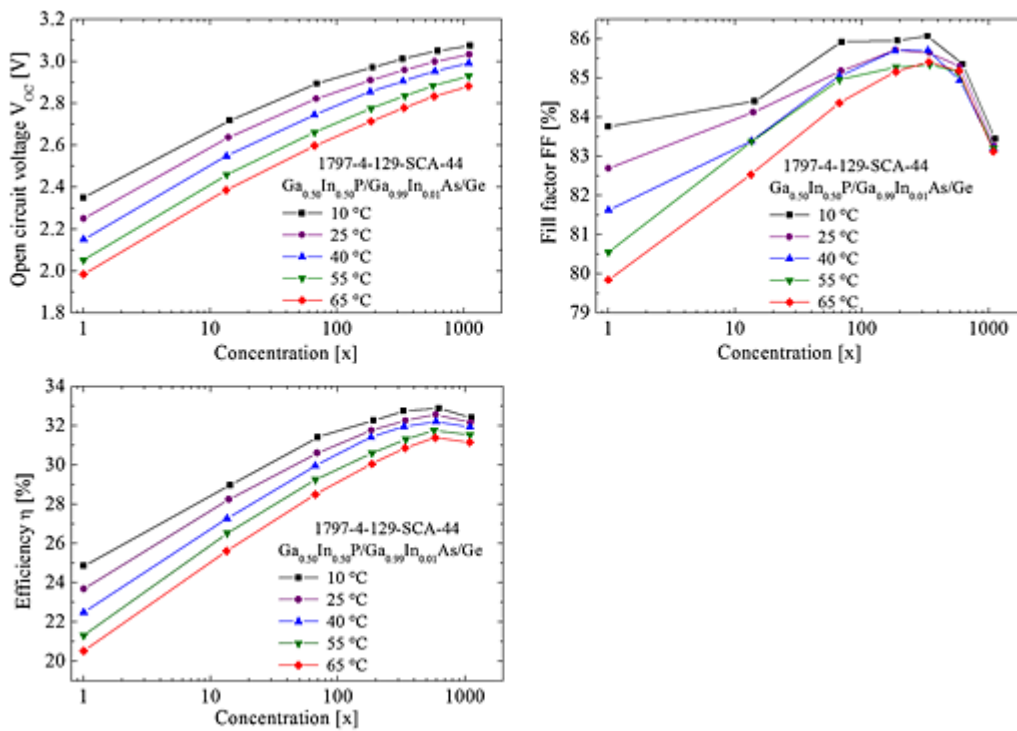
1249



1250

1251

Fig.26. The module's electrical parameters dependent on temperature [82].



1252

1253

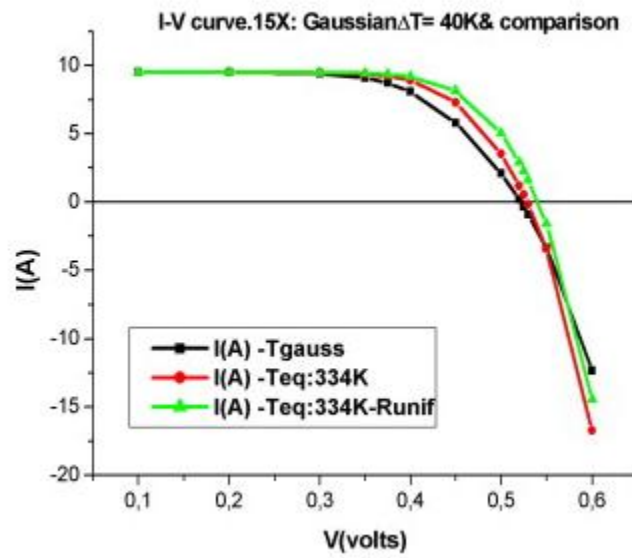
Fig.27. Open circuit voltage  $V_{oc}$ , fill factor  $FF$  and efficiency  $\eta$  of the

1254

$Ga_{0.50}In_{0.50}P/Ga_{0.99}In_{0.01}As/Ge$  triple-junction cell at different temperatures [84].

1255

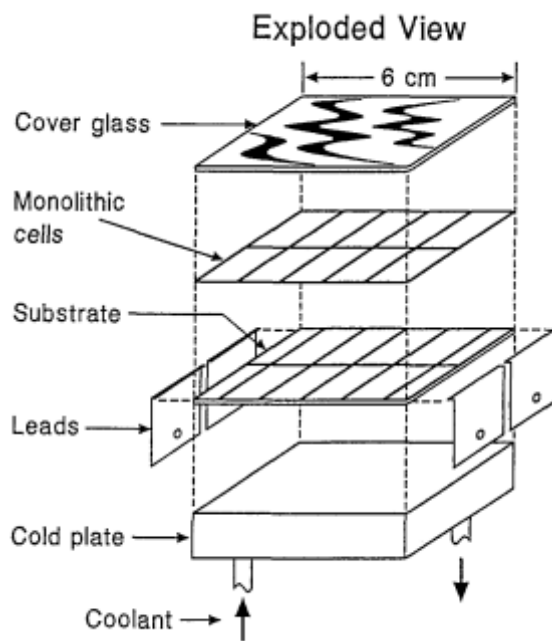
1256



1257

1258

Fig.28. Comparison of the  $I-V$  curves of a cell under three conditions [45].



1259

1260

Fig.29. Cooling structure of the PV module [95].

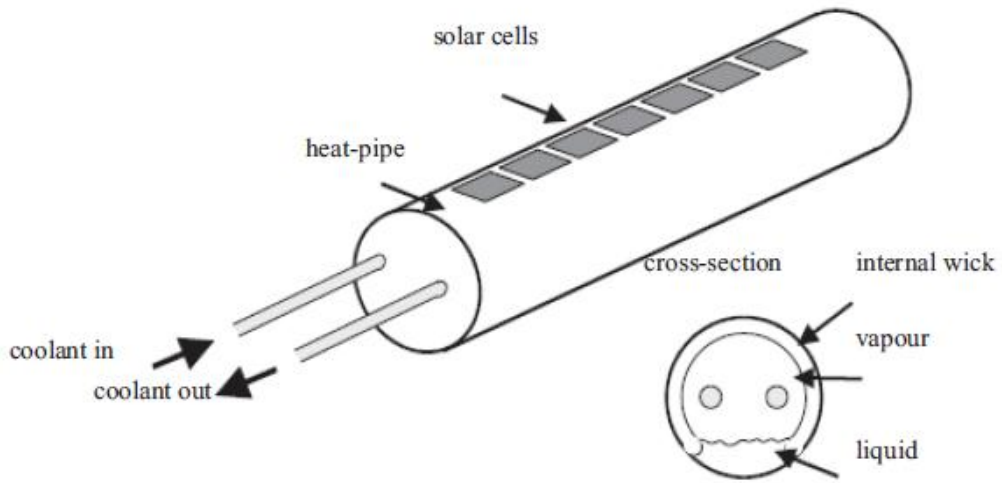
1261

1262

1263

1264

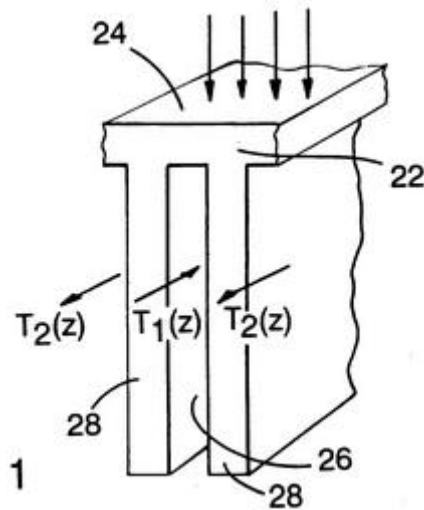
1265



1266

1267

Fig.30. Heat pipe based cooling system [90].



1268

1269

Fig.31. A cross-sectional view of a portion of the micro-channel heat sink [101].

1270

1271

1272

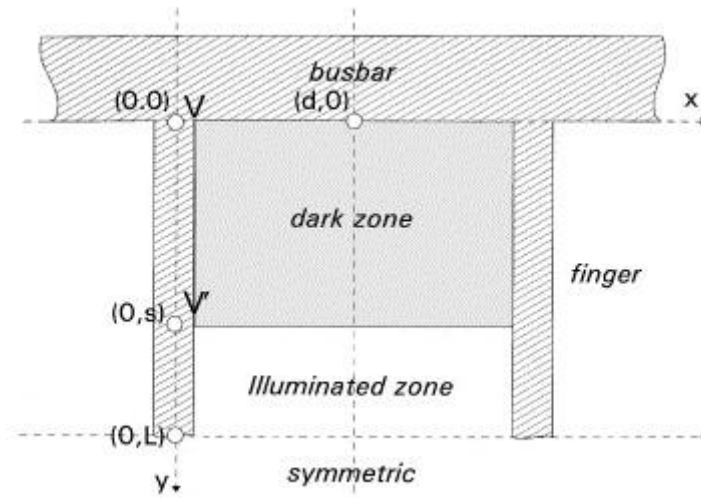
1273

1274

1275

1276

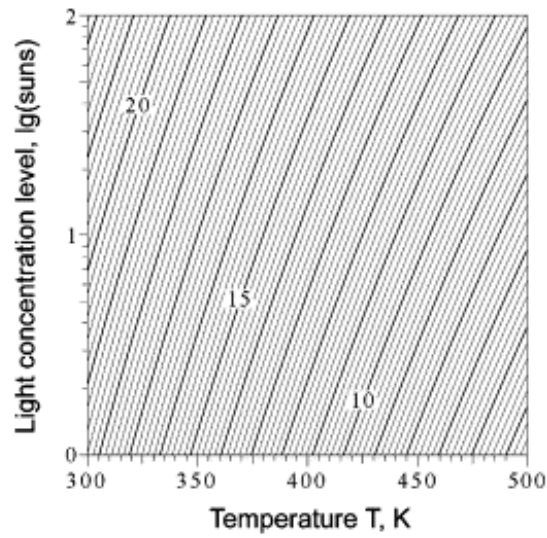
1277



1278

1279

Fig.32. Schematic of the cell grid for series resistance calculations [110].



1280

1281

Fig.33. Efficiency of solar cells under simultaneous influence of temperature and

1282

solar concentration [81].

1283

1284 Table 1. The causes of non-uniform illumination [31], [35], [37] and [38].

1285

Causes	Concentrator design	Relative position of the solar cell and the sun	Other factors
1	Unreasonable design	Improper tracking system	Shading
2	Material	Deviation of optics and cell	Spectral response
3	Profile errors	(the cell isn't in the right	
4	Manufacturing problems	position of the optics' absorbers)	

1286

1287 Table 2. Cell parameters under 12 suns uniform illumination [32].

IV characteristics for cell simulated under 12 suns uniform illumination

$I_{sc}$	20.97A
$V_{oc}$	0.65V
$FF$	0.79
Efficiency	19.25%

1288

1289 Table 3. Comparison between uniform and non-uniform illumination.

Researcher	Type of cell	Type of PV system	Cell parameters				Key findings
			$I_{sc}$	$V_{oc}$	$FF$	$\eta$	
Coventry [39]	monocrystalline silicon	LI, CPV90×, middle third	-	6.5 mV reduction	-	1.2% reduction	Reductions are unavoidable without secondary

		of cell					flux modifier.
<b>Katz, et al.[41]</b>	GaInP2/GaAs/Ge triple-junction uniform front metallization	LI, illuminated fraction: 0.00785	no obvious change	0.09V under $P_m = 8W$	0.2 reduction under $P_m = 8W$	8% reduction under $P_m = 8W$	The position of the LI on cell have little influence on $FF$ .
<b>Manor A, et al.[42]</b>	organic cell	LI, non-CPV to CPV10×	increase, linear growth	decrease, reduction almost be same	decrease, largest at CPV1×, 0.3	decrease, largest at CPV1×, 2%	LI of different part over the cell area gave identical results.
<b>Franklin and Coventry [31]</b>	distributed resistance, cell model	Gaussian illumination, Average concentration ratio of 22.7	-	5mV reduction	-	0.5% reduction	Reductions become larger with increasingly centralized illumination profile.
<b>Mellor, et al.[32]</b>	two-dimensional, front surface currentflow, cell model	Gaussian illumination, mean illumination intensity CPV12×	-	0.007V reduction under PIR of 10	0.06 reduction under PIR of 10	1.7% reduction under PIR of 10	Increasing the number of fingers of the front contact can mitigate the decrease in each parameters.
<b>Domenech-Garrret [45]</b>	silicon monocrystalline ASE solar cell	Gaussian illumination, CPV15×	-	10mV reduction	0.01 reduction	-	The illumination profile spoils the fill factor.
<b>Herrero, et al.[44]</b>	multi-junction	Gaussian illumination	-	-	0.003 reduction under PAR of 4.01	-	Reduction is due to an increase in series resistance and lead to efficiency decline.
<b>Algora [46]</b>	3-D, distributed circuit units, cellmodel	average illumination CPV1000×	-	slight decrease	0.003 under good contact, 0.059 under medium contact	0.4% under good contact, 1.63% under medium contact	The worse the quality of the front contact, the greater the decrease in both $FF$ and $V_{oc}$ .
<b>Goma, et al.[47]</b>	c-Si	CPV, different incident light intensity	-	-	0.03 reduction	-	To reduce the effect of concentration distribution, it is necessary to control the $R_s$ .
<b>Araki, et al.[48]</b>	AlGaAs/GaAs 2-junction	Gaussian illumination CPV500×	-	-	significant reduction	-	$FF$ can be partially recovered by chromatic

<b>Pozner, et al.[50]</b>	monolithic silicon, vertical multi-junction	non-uniform, by parabolic dish concentrator	-	-	-	-	aberration. Dense array CPV modules based on VMJ cells connected in parallel feature very low sensitivity to non-uniform illumination.
---------------------------	---	---	---	---	---	---	---

1290

1291 Table 4. Comparison between uniform and non-uniform temperature.

Researchers	Type of cell	Type of PV system	Cell parameters				Key findings
			$I_{sc}$	$V_{oc}$	$FF$	$\eta$	
<b>Meneses -Rodríguez, et al.[85]</b>	crystalline silicon	CPV, elevated temperature	no obvious change	0.4 V reduction from 300K to 500K	0.25 reduction from 300K to 500K	6% reduction from 300K to 500K	Reduction of efficiency is mainly due to the reduction of the $V_{oc}$ and $FF$ , the influence of the current value could be neglected.
<b>Nishioka, et al.[56]</b>	InGaP/InGaAs/Ge triple-junction	CPV, elevated temperature	slight increase under 200 suns	0.4 V reduction under 200 suns	0.04 reduction under 200 suns	3% reduction under 200 suns	This solar cells have an advantage over crystalline-silicon solar cells under high-temperature conditions.
<b>Peharz, et al.[86]</b>	GaInP/GaInAs/Ge triple-junction	CPV, elevated temperature	increase of 0.13A%/K	decrease linearly by 0.18V%/K	decrease of 0.16%/K	decrease of 0.1%/K	The temperature dependence of Fresnel lenses and thermal expansion of the CPV modules will reduce the positive short circuit current.
<b>Siefer, et al.[84]</b>	GaInP/GaInAs/Ge triple-junction	CPV, elevated temperature	-	-	-	decrease	The main reason for the decline is that the open circuit voltage will



---

<b>Domenech-Garret [45]</b>	silicon monocrystalline ASE solar cell	Gaussian temperature profile	-	18mV reduction	0.03 reduction	-	decrease when operated at a high temperature under concentration. The increasing and uneven temperature both have an effect on cell parameters.
-----------------------------	--	------------------------------	---	----------------	----------------	---	--

---

1292

1293

1294

1295

1296

1297

1298

1299

1300

1301

1302

1303

1304

1305

1306

1307

1308

1309

1310 Table 5. Comparison of different cooling methods

Types of cooling method	Characteristics	Researchers	Type of system	Working principle	Key findings
Air cooling technology	Air can take heat away to keep cell's temperature in a low level by convection passively or actively from the back of the solar cell.	Hussain, et al.[93]	Enerworks Heat Safe (EHS) residential solar collector integrated with a back mounted air channel.	Ambient air was introduced between the absorber plate and the back insulation thereby allowing the natural convection cooling of the collector absorber plate	A solar collector integrated with a well designed back mounted air cooling channel and a control valve at the outlet opening would be able to provide suitable heat transfer rates
		Araki, et al. [94]	500 X concentrator module made by printed epoxy and copper sheet on aluminum plate.	Aluminum plate was used to attached to the solar cell which diffused heat at the concentrated region and transferred the heat into the air.	Good thermal contact between solar cell and aluminum plate is the key to keep the concentrator low temperature.
Water cooling technology	Water cooling offers a good performance because of its high convection coefficient and thermal capacity.	Verlinden, et al [95]	Monolithic silicon concentrator module consisted of 10 cells	Monolithic PV module was mounted on a cold plate of the same size, and the heat generated by the solar cells was absorbed by the coolant in the cold plate.	The module got a 0.8% growth of efficiency when operated at 25°C compared to 39°C.
		Verlinden etal. [96]	250 X reflective parabolic dish whose receiver is composed of 16 modules, each with 24 series-connected silicon solar cells.	The PV modules were laminated onto the ceramic substrate and ceramic substrate was attached on a water cold plate for active cooling.	The cell efficiency can reach 24% and the system comprehensive energy utilization efficiency can surpass 70%.

<b>Heat pipe cooling technology</b>	Heat pipes are high heat flux transformation devices and has a good temperature performance at the same time. One end is stick to the solar cell and absorb the heat, and another is exposed to cooling environment	Tarabsheh, et al. [99]	PV string with the cooling pipes beneath it.	The module is cooled by a fluid flowing through pipes underneath the PV module backside. The fluid serves as both heat sink and solar heat collector.	Implementing cooling pipes underneath each PV string improves the performance of the PV cells
<b>Micro-channels technology</b>	Small size and it can directly cool the millimeter level heat source, but the temperature gradient and the pressure loss is large.	Missaggia and Walpole [101]	Alternating-channel-flow micro-channel heat sink.	The micro-channel heat sink was used by making the thermal contact between the device and the heat sink and the coolant will absorber and remove the heat.	It can reduce the surface temperature variations compared to a conventional one with one-directional flow.
		Yang and Zuo [102]	CPV cells with multi-layer manifold microchannel cooling system.	The water was filled in the manifolds, and then was forced to flow into microchannels and took away the heat from heat sources.	surface temperature difference of the CPV cell was below 6.3 C and multi-layer manifold microchannel had a heat transfer coefficient of 8235.84 W/m <sup>2</sup> K and its pressure drop was lower than 3 kPa.

<b>Liquid immersion cooling technology</b>	Liquid immersion cooling involves the immersion of solar cells directly into the circulating liquid and the heat is absorbed by the circulating coolant form both the front and back surface of the PV string [7].	Liu, et al. [103]	Common silicon cells 2CR immersed into a dielectric liquid.	The direct-contact heat transfer between both the front and back surfaces of the module and the dielectric liquid.	The temperature distribution of cell module is fairly uniform within 3 °C under turbulent flow mode under the condition that heat is removed from both the back and front of the panel in a dielectric fluid.
<b>Impingement jet cooling technology</b>	Impingement jet cooling technology can obtain the low thermal resistance and has been widely used in many industrial fields at present [95].	Royne, et al. [105]	Arrays of densely packed PV cells.	Liquid was drained in a direction normal to the heated surface around the edges of the central array of jets.	A broad optimal operating region for any system of photovoltaic cells and cooling device at a given illumination level was found.
<b>Phase change material technology</b>	PCMs, also called latent heat storage devices with a constant temperature during the phase change process which can result in the PV surface to be remained at uniform temperature.	Hasan, et al. [106]	Building integrated photovoltaics.	Excess heat is absorbed by PCMS during melting change in phase from solid to liquid at a stable transition temperature thus to regulate the temperature of the PV.	A maximum temperature reduction of 18 °C was achieved for 30 min while 10 °C temperature reduction was maintained for 5 h at 1000 W/m <sup>2</sup> insolation.
		Sharma, et al [107]	Building-Integrated Concentrated Photovoltaic (BICPV) systems	Excess heat is absorbed by PCMS during melting change in phase from solid to liquid at a stable transition temperature thus to regulate the temperature of the PV.	An increase in relative electrical efficiency by 7.7% with PCM incorporation. An average reduction in module centre temperature by 3.8 °C was recorded in the BICPV-PCM integrated system as compared to the naturally ventilated system without PCM.

1311

1312